DOT/FAA/CT-83/16

Application of Thermochemical Modeling to Aircraft Interior Polymeric Materials II - Multilayered Seat

W. Dokko
K. Ramohalli

Prepared by
Jet Propulsion Laboratory
California Institute of Technology
Pasadena, California

October 1983

Final Report

US Department of Transportation
Federal Aviation Administration
Technical Center
Atlantic City Airport, N.J. 08405

FSS 000289 R

NOTICE

This document is disseminated under the sponsorship of the Department of Transportation in the interest of information exchange. The United States Government assumes no liability for the contents or use thereof.

The United States Government does not endorse products or manufacturers. Trade or manufacturer's names appear herein solely because they are considered essential to the object of this report.

Technical Report Documentation Page

1. Report No.	2. Government Accession No.	3. Recipient's Catalog No.
DOT/FAA/CT-83/16		

4. Title and Subtitle	5. Report Date
Application of Thermochemical Modeling to Aircraft Interior Polymeric Materials II - Multilayered Seat Cushions	October 1983
	6. Performing Organization Code
7. Author(s) Won Dokko and Kumar Ramohalli	8. Performing Organization Report No. JPL D-955
9. Performing Organization Name and Address Jet Propulsion Laboratory California Institute of Technology Pasadena, California 91109	10. Work Unit No. (TRAIS)
	11. Contract or Grant No. 181-350-100
	13. Type of Report and Period Covered
12. Sponsoring Agency Name and Address U.S. Department of Transportation Federal Aviation Administration Technical Center Atlantic City Airport, New Jersey 08405	June 1981 - May 1982
	14. Sponsoring Agency Code

15. Supplementary Notes

16. Abstract

This report summarizes the results from a twelve-month study of applying thermochemical modeling to multilayered polymeric materials, passenger aircraft seat cushions. The use of fire-blocking layer(s) between the foam cushion and the covering fabric has been studied extensively to minimize fire hazards from aircraft seats. The objectives of this work are to expand the thermochemical model for the multilayered materials and to experimentally verify theoretical predictions. First, the thermochemical model is extended to any number of multilayered materials, by applying the same analysis technique used in the previous work. The additional constraints of temperature and heat flux continuities at every interface are also applied. A computer program is developed to predict burning behavior of seat cushion systems with and without a fire-blocking layer. Second, a series of tests burning seat cushions with and without a fire-blocking layer are conducted in a modified NBS Smoke Density Chamber. The chamber was supplemented with a multichannel recorder/multiple thermocouples and a weight-measuring device to determine temperature profile and to continuously monitor weight loss, respectively. The results indicate that the predicted temperature profiles are in very good agreement with the experimentally determined ones, and that the same effectiveness of the fire-blocking layers are predicted as those of actual weight loss measurements. It is, however, observed that the formation and presence of a void inside of the polyurethane foam seem to cause the over-prediction of the temperature profile and under-prediction of the weight loss (compared to the case when the void is small or nonexistent).

17. Key Words	18. Distribution Statement
Thermochemical modeling; fire safety, aircraft interior materials, multilayers, fire blocking layer, seat cushion, temperature profile, weight loss	This document is available to the U.S. public through the National Technical Information Service, Springfield, Virginia 22161

19. Security Classif. (of this report)	20. Security Classif. (of this page)	21. No. of Pages	22. Price
Unclassified	Unclassified		

Form DOT F 1700.7 (8-72)

NOTICE

This document is disseminated under the sponsorship of the Federal Aviation Administration, U. S. Department of Transportation in the interest of information exchange. The United States Government assumes no liability for the contents or use thereof.

The United States Government does not endorse products or manufacturers. Trade or manufacturers' names appear herein solely because they are considered essential to the object of this report.

PREFACE

The work described in this report was performed by the Jet Propulsion Laboratory (JPL), California Institute of Technology (Caltech), and was sponsored by the Federal Aviation Administration (FAA) through an agreement with the National Aeronautics and Space Administration (NASA). The authors would like to thank Dr. Thor Eklund, the FAA Project Manager, Messrs. Constantine Sarkos, Wayne Howell, and Richard Kirsch of the FAA and Allen Tobiason of NASA for their suggestions and support.

TABLE OF CONTENTS

LIST OF ILLUSTRATIONS

LIST OF TABLES

NOMENCLATURE

B	Pre-exponential constant for thermal degradation of polymer (sec^{-1})
c	Specific heat (cal gm^{-1} $°C^{-1}$)
D	Heat of degradation (cal gm^{-1})
E	Activation energy for thermal degradation of polymer (cal $mole^{-1}$)
FS	Remaining number of monomer units of degraded polymer
k	Thermal conductivity (cal cm^{-1} sec^{-1} $°C^{-1}$)
N	Remaining number of polymer bonds normalized with respect to the number in the unaffected state
q	Heat flux (cal cm^{-2} sec^{-1})
r	Linear regression rate of polymer solid (cm sec^{-1})
R	Universal gas constant (cal g-$mole^{-1}$ K^{-1})
t	Time (sec)
T	Temperature (K)
w	Weight (gm)
x	1-dimensional coordinate, i.e., depth from surface (cm)
ρ	Density (gm cm^{-3})
λ	The normalized regression rate eigenvalue ($\propto 1/r^2$)

Subscripts

1, 2, 3	Pertaining to each of multilayers
s	Front (hot side) surface of a layer
c	Rear (cold side) surface of a layer
o	Undisturbed state
L	Thickness of a layer

Superscripts

+, -	A point immediately beyond and before, respectively

EXECUTIVE SUMMARY

The purpose of this effort was the evaluation of the fire performance of seat blocking layers for urethane seat cushions. Because urethane cushions have been demonstrated as highly flammable under aircraft post-crash fire conditions, seat blocking layers have been proposed as a method of protecting the urethane from involvement with the fire. Many hypothesis have been proposed to explain the manner in which fire blocking layers achieve their desired effect, but such hypothesis have not been verified in any quantitative sense.

A condensed phase thermochemical modeling theory previously developed for single component aircraft materials was modified to handle multi-layered materials. The model is based on analytical heat and mass transfer relationships. Required experimental inputs into the model are material thermal properties typical of heat transfer calculations. Additionally, the analysis technique known as thermogravimetric analysis is used to establish the parameters that describe the thermal breakdown of the plastic material when exposed to fire.

Parallel to this analytic work, experimental tests were conducted on sample blocking layer materials in a modified smoke chamber of National Bureau of Standards (NBS) variety. The samples were exposed to specified heating rates and both their weight loss and thermal behavior were measured. This measured behavior is compared with the predictions of the analytic evaluation.

The findings of the investigation are that the thermochemical model can predict the effectiveness of seat blocking layers within a limited range of fire exposure conditions. Additionally, the NBS Smoke Chamber is a useful small scale test for screening candidate seat blocking layers.

1. INTRODUCTION

Aircraft cabin fire safety has been one of the major research and development activities for the Federal Aviation Administration (FAA) for more than 30 years in the past (reference 1). The reasons for such a long-term commitment are the fatalities observed, unique environment in an aircraft (such as small space, high density of people, limited access for egress, etc.), and the complexity in fire phenomenon itself.

In general, fire potential in a passenger aircraft can be due to jet fuel and cabin interior materials. However, a fire involving only the interior materials can occur in-flight or on the ground. In the case of a postcrash fire, a jet fuel fire can ignite interior materials, and the hazards arise from interaction of the fuel fire with interior materials (reference 2).

As planned earlier (reference 4), this work is on the prediction of material burning phenomena through condensed phase thermochemical modeling, and does not involve gas dynamic modeling. These two approaches may well be bridged in the future (reference 3) with sufficient progress.

Among the cabin interior materials such as carpet, seats, window screens, sidewall panels, ceiling and partitions, one of the most flammable materials, seat cushion, is the subject of the current work. Previous work, last year, (reference 4) was on wool carpet and polyurethane foam treated as single layer materials.

In this work, the seat is treated as a system of multilayered polymeric materials, consisting of a seat cover fabric, polyurethane foam cushion, and a fire blocking layer.

In addition to analytically predicting the burning behavior of multilayered systems as a function of heat flux and layers' thicknesses, burning tests are conducted in a modified NBS density chamber to verify the temperature profile and weight losses predicted by the model.

2. THEORETICAL

The thermochemical model used in this work is an extension of the model developed earlier for a single-layered material. As a matter of fact, the approach used in predicting the burning rate of wool carpet with a char layer on its top (reference 4) is a particular form of such an extension. Another earlier work (reference 5) applied to the study of burning rate of composite materials is also referenced for the generalized extension.

(a) The Applicability of the Steady-State Model

There are two aspects of this time-independent model which should be recognized. One is the coordinate transformation (a la Spalding (reference 11)) that enables us to treat the regressing surface as if it were stationary and the other is the more fundamental argument on the relative time scales.

(1) The assumption of time-independent degradation enables one to see that d/dt can be written as $r \cdot d/dx$. This transformation, the authors believe, was first introduced in combustion theory by Brian Spalding (reference 11) in his treatment of laminar flame propagation in premixed gases. The point is that the "transient" propagation can be viewed as steady-state in another coordinate frame.

(2) In any case, the assumption $\partial/\partial t \equiv 0$ implies that the characteristic heat transfer time is small compared to the characteristic "flow" or thermal wave propagation time. The time needed for the establishment of the fully developed temperature profile in the solid is, of course, infinity from the first order nature of the equation's; recall

$$(T_x - T_o)/(T_{xs} - T_o) = 1 - \exp(-\alpha t/x^2)$$

where T_x is the temperature at any depth x (from the surface), T_o is the initial temperature, T_{xs} is the steady-state temperature at depth x, α is the thermal diffusivity

($\equiv k/\rho c$), t is the time. Thus the time-independence assumption in our treatment relies on a small value for the characteristic time L^2/α for its validity. In the case on hand, the following approximate numbers lend credence to this approach. Typically $\alpha = 10^{-3}$ cm^2/sec. The "characteristic" thermal depth, i.e., the distance from the surface to reach 1/e of the full temperature difference is 0.2 cm (for example from figure 11, first plot) at 120 seconds (2 min.); or

$$t \frac{\alpha}{x^2} \approx 3.0$$

leading to

$$1 - \exp(-\alpha t/x^2) > 0.9$$

Thus the steady-state assumption is valid in our case of heating rates.

(b) Mathematical Formulation

As in the previous work, the geometry under consideration is one-dimensional, and the steady-state condition is assumed throughout the analysis. The following mathematical analyses for a multilayered system are divided into three parts: the first part is for the case where a single-layered material is so thick that the rear surface (cold side) temperature is undisturbed; the second part is the same as above except that the rear surface temperature has been raised substantially, and the third case is the extension for a layer which is on top of the above two layers and has as many colder layers underneath it as determined by the configuration.

In all three cases, the governing equation for each layer is the same, that is,

$$k \frac{d^2T}{dx^2} + \rho cr \frac{dT}{dx} = D\rho NB \exp(-E/RT) \qquad (1)$$

The right-hand side of this equation is the heat sink term corresponding to the first-order degradation reaction described by

$$-\frac{1}{N}\frac{dN}{dt} = B \exp(-E/RT) \qquad (2)$$

The symbol N represents the number of remaining bonds per unit mass, normalized with respect to that of fresh, unburned material. The symbol D, the heat of degradation, is "positive" when the degradation reaction is endothermic and "negative" when exothermic.

The boundary conditions, however, are different for each case.

(1) First case, i.e., $T = T_0$ at $x = \infty$

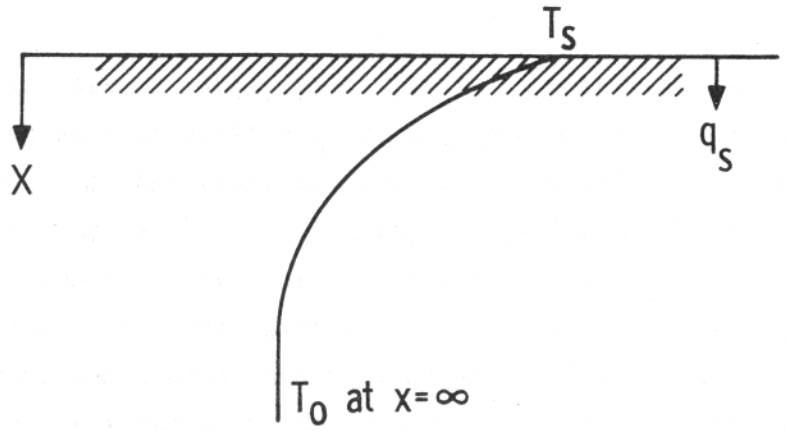

Figure 1. Geometry considered in the first case where $T = T_0$ at $x = \infty$

When the rear surface (cold side) temperature is undisturbed, the boundary conditions for equations (2) and (3) are, respectively,

$$T = T_s \quad \text{at} \quad x = 0 \qquad (3)$$
$$T = T_o \quad \text{at} \quad x = \infty$$

$$N = 1 - \frac{1}{FS} \quad \text{at} \quad x = 0 \qquad (4)$$
$$N = 1 \quad \text{at} \quad x = \infty$$

The symbol FS stands for fragment size, an average number of monomer units of degraded polymer.

Assuming constant values of material properties, the solution for r, surface regression rate, has been obtained (reference 6) by singular perturbation methods with matching the solution for the inner (surface) and outer (deep solid) regions. For the steady state system, r is given as:

$$r = \sqrt{\frac{(k/\rho c)\, B \exp\left(-E/RT_s\right)}{\left(\frac{E}{RT_s}\right)\left(\frac{T_s-T_o}{T_s}\right)\left[\left\{1 + \frac{D}{c(T_s-T_o)}\right\} \ell n\left(\frac{FS}{FS-1}\right) - \frac{D}{c(T_s-T_o)FS}\right]}} \qquad (5)$$

And the integration of equation (1) will show that the conductive heat flux at the hot surface is

$$q_s = \rho r \left[c\,(T_s-T_o) + {}^{D}/_{FS}\right] \qquad (6)$$

if there is zero heat flux at the rear surface. Thus, all the thermal energy flowing into the layer can be said to be totally consumed within the layer.

(2) Second Case, i.e., $T = T_c$ ($> T_o$) at $x > 0$

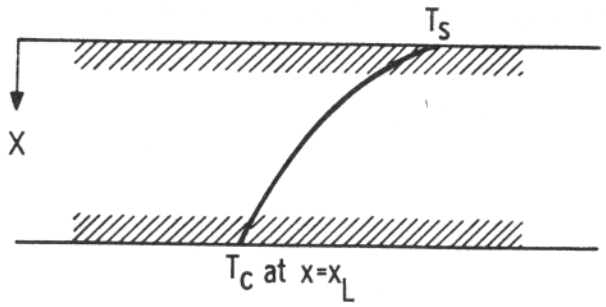

Figure 2. Geometry considered in the second case where $T = T_c$ at $x = x_L$

This is the case when the front (hot) and rear surface temperatures of a layer are substantially higher than the unperturbed condition of T_o. The governing equations are the same as above, i.e., equations (1), (2), and the boundary conditions are

$$\begin{aligned} T &= T_s \quad \text{at} \quad x = 0 \\ T &= T_c \quad \text{at} \quad x = x_L \end{aligned} \tag{7}$$

$$\begin{aligned} N &= 1 - \frac{1}{FS_s} \quad \text{at} \quad x = 0 \\ N &= 1 - \frac{1}{FS_c} \quad \text{at} \quad x = x_L \end{aligned} \tag{8}$$

Assuming that T_c is close to T_s, that is

$$\frac{T_s - T_c}{T_s - T_o} < 0.1 \tag{9}$$

the solution for r is given by

$$r = \sqrt{\frac{(k/\rho c)\, B \exp\,(-E/RT_s)}{\lambda \left(\frac{E}{RT_s}\right)\left(\frac{T_s - T_o}{T_s}\right)}} \tag{10}$$

The details of this derivation is shown in appendix A.

The integration of equation (1) in the region between the front and rear surfaces will give the net heat flux, that is, the incoming heat flux at the front surface minus the one at the rear surface.

$$q_{net} = \rho r \left[c\,(T_s - T_c) + D\left\{ \frac{1}{FS_s} - \frac{1}{FS_c} \right\} \right] \qquad (11)$$

In other words, the above equation determines the net heat consumed within the layer volume, as sensible heat and heat of degradation.

(3) Third Case of a multilayered system

In the above two cases, the analyses are for a homogeneous single layer for which thermal, physical and chemical properties are constant and uniform in every part of the layer. If a system consists of more than one material, like the example of a cover fabric - blocking layer - foam, those properties are widely different and hence will be treated as a multilayered system.

Strictly speaking, even a single component material should be treated as a multilayered system, if the temperature drop from the front to the rear surface is so large that the thermal, physical and chemical properties can not be considered constant and uniform within the layer.

In other words, when a material of certain thickness is burning, it is a multilayered system from the view point of thermochemical behavior. As shown later, B and E of any single material employed in this study do not remain constant over the temperature range of interest but vary considerably.

For this reason, each component material of a multilayered seat cushion system is in itself considered multilayered, divided by temperatures at which any of the thermal and/or thermochemical properties changes substantially. Hence, the total number of layers, i.e., thermochemical layers, of a seat cushion system become equal to the sum of the thermochemical layers of each component material.

For the ease of analysis, first suppose that a system of three layers is undergoing pyrolysis reaction, as depicted in figure 3. The same analysis can be extended to any system with more than three layers with the change in subscripts.

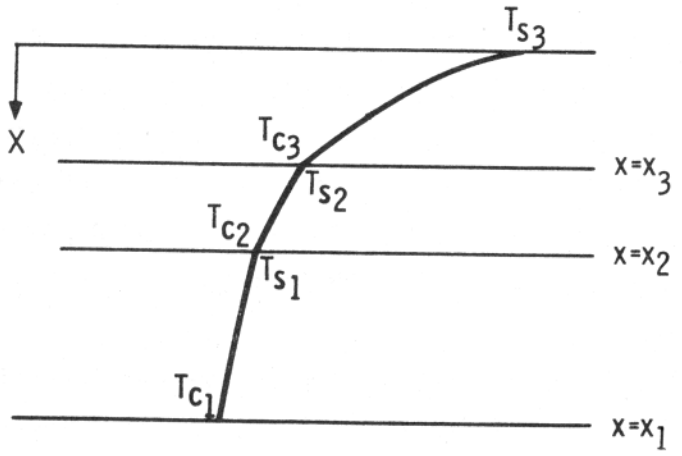

Figure 3. Geometry of the third case, a three-layered system

The conductive heat flux at the top surface (x=0) should be the sum of all the energy, i.e., the sensible heat and the heat of degradation, required for the pyrolysis of all three layers in this 1-D approximation. The energy required for each individual layer is shown in equation (6) or equation (11). Then, the incoming heat flux at the top surface of the first, second, and the third layer is, respectively,

$$-k_3 \left.\frac{dT}{dx}\right|_{x=o^+} = \rho_3 r_3 \left[c_3 (T_{s_3} - T_{c_3}) + D_3 \left(\frac{1}{FS_{s_3}} - \frac{1}{FS_{c_3}}\right)\right]$$
$$+ \rho_2 r_2 \left[c_2 (T_{s_2} - T_{c_2}) + D_2 \left(\frac{1}{FS_{s_2}} - \frac{1}{FS_{c_2}}\right)\right] \quad (12)$$
$$+ \rho_1 r_1 \left[c_1 (T_{s_1} - T_{c_1}) + D_1 \left(\frac{1}{FS_{s_1}} - \frac{1}{FS_{c_1}}\right)\right]$$

$$-k_2 \left.\frac{dT}{dx}\right|_{x=x_3^+} = \rho_2 r_2 \left[c_2 (T_{s_2} - T_{c_2}) + D_2 \left(\frac{1}{FS_{s_2}} - \frac{1}{FS_{c_2}}\right)\right]$$
$$+ \rho_1 r_1 \left[c_1 (T_{s_1} - T_{c_1}) + D_1 \left(\frac{1}{FS_{s_1}} - \frac{1}{FS_{c_1}}\right)\right] \quad (13)$$

and

$$-k_1 \left.\frac{dT}{dx}\right|_{x=x_2^+} = \rho_1 r_1 \left[c_1 (T_{s_1} - T_{c_1}) + D_1 \left(\frac{1}{FS_{s_1}} - \frac{1}{FS_{c_1}}\right)\right] \quad (14)$$

There are however, two kinds of physical constraints applied at each interface. The first kind is that

$$\begin{aligned} T_{c_3} &= T_{s_2} \\ T_{c_2} &= T_{s_1} \end{aligned} \quad (15)$$

and the second is that

$$\begin{aligned} -k_3 \left.\frac{dT}{dx}\right|_{x=x_3^-} &= -k_2 \left.\frac{dT}{dx}\right|_{x=x_3^+} \\ -k_2 \left.\frac{dT}{dx}\right|_{x=x_2^-} &= -k_1 \left.\frac{dT}{dx}\right|_{x=x_2^+} \end{aligned} \quad (16)$$

The above two conditions are to satisfy the continuity of temperature and heat flux at interfaces.

In the expression of equations (12), (13), or (14), each r is implicitly defined. In other words, the heat fluxes at the upper and lower boundaries of each layer are used in obtaining the r of that layer (as shown in appendix A), and are in turn used to define the heat fluxes [as shown in equations (12), (13), and (14)]. This poses no problem in actual calculations since any iterative method leads to fairly rapidly converging answers. The significance of this fact is, however, that the calculation of r's should proceed layer by layer, from the rear (coldest) to the front (hottest), or from the front to the rear.

(c) Computer Program

Based on the theory discussed above, two computer programs are developed and listed in appendix B. The first program, (Computer Program A) takes the interfacial temperatures as the input data, and the second (Computer Program B) takes the temperature and the conductive heat flux at the front surface as its input. The choice among these two programs is dictated firstly by the available boundary conditions, and the other may be used as a complementary to obtain additional information.

(d) The Overall Logic and Characteristics of the Model

The model was originally developed to account for the host of inconsistencies in polymer degradation and burning rate data. The most important distinguishing characteristics are the recognition that the mean molecular weight of the vaporizing molecules need not be equal to the monomer molecular weight. Instead, a vapor pressure equilibrium criterion was used to unambiguously specify the mean molecular weight at the surface. This procedure not only removed an

annoying arbitrainess at the surface, but also checked well, in terms of results, with data from various classes of polymer combustion. Under the assumption of first order Arrhenius kinetics for the degradation of the subsurface polymer, the model, in its present state, cannot handle cases where extensive degradation beyond the monomer stage takes place before vaporization. This is not as severe a limitation as it may seem. It has been documented (e.g., see Stanley Martin, X Symposium (International) on Combustion) that many of the the degradation reactions actually take place after the major precursors (i.e., products of partial degradation) have left the surface.

The model also assumes that the thermal wave front moves at a uniform speed in the solid. This thermal wave can be associated with the mean surface (and hence the wave speed is indeed the burning rate or "regression rate") only when all of the solid (condensed phase) gets transformed into vapor. This is indeed the case in the burning of simple plastics (e.g., plexiglas, polyethylene, polyurethane . . .). In the case on hand, substantial charring occurs indicating that the familiar "regression rate" needs careful interpretation. For example, it is a familiar fact that in wood burning the reactive portion (cellulose and hemicellulose) leaves the solid framework of lignin char. In such cases of charring solids, the regression rate is more appropriately associated with the velocity of the thermal wave in the wake of which the reactive portion gets vaporized and leaves the char. Thus, it may appear that the surface is not really regressing in the physical sense, although the reactive portion is. Up to this point, the interpretation of the regression rate of this model is clear. The interpretation gets more complex as multilayered materials are concerned. Hence, clearly, the regression rate of the II layer, if interpreted literally, will give rise to a "void" or separation between the bottom of the I layer and the initial position of the II layer top surface. However, the complexity is removed when one recognizes that the regression meant here is really the movement of the thermal wave in the solid layers while the char framework (end

product of the degradation) is stationary in the laboratory frame of reference. The appropriate way of handling this situation mathematically is to keep the density of the material ρ as a variable. For example, ρ_{final} would not equal zero but would equal the char density which itself is equal to the $(\rho_{initial} - \rho_{reactive})$.

With this interpretation, the regression rate r is really always associated with the mass flux ρr where ρ is not the density of the solid but is only the density of the reactive portion of the solid. However, in the evaluation of the properties such as the thermal diffusivity of the reacting solid, the full density has to be used. Also, the heat transfer through the char is characterized by a thermal conductivity coefficient of the char, and the volatiles convection (flow) through the char. This has been highly simplified in the present analysis which considers the temperature to be constant (and equal to the temperature of the bottom surface of the immediate layer above). Clearly, more work is needed to mathematically incorporate into the model, the realistic char formation, flow and heat transfer.

The "void" that is mentioned in the experimental portion is not the same on this void or separation. Experimentally it is found that the mechanical movement of the volatiles frequently causes a void in the assembly and physical separation of layers. This is a very complex process mathematically.

Considering all of these complexities, the agreement between the theory and experiments in this study is thought to be encouraging.

3. EXPERIMENTS

The experiments of this work consist of two parts; one is to obtain the kinetics constants using thermogravimetry (TG) and the other is, through actual burning tests, to determine the temperature profile established within a seat cushion assembly and the weight loss during pyrolysis. The experimental results are compared with the model predictions.

(a) Thermogravimetry

This experiment heats up a small sample suspended inside a furnace and records the weight change as a function of temperature. The kinetics constants, B and E, are deduced then from an Arrhenius plot, a plot of log $\{(1/w) \cdot -(dw/dt)\}$ versus reciprocal of absolute temperature $(1/T)$.

It was known from previous work (reference 4) that the ambient gas composition, more precisely the oxygen concentration, affects the kinetics constants. This is a very important point. It has long been recognized that even minor ($\sim$1%) concentrations of certain oxidative species can significantly alter (by almost an order-of-magnitude) the degradation rates of polymers. And yet no detailed study seems to be available in this area. One study that addressed this question specifically stopped short of actually demonstrating the effects but had to make valid (but indirect) deductive arguments to point the importance. In any combustion situation, especially with flow of gases over the surface (a very common aircraft fire scenario), the oxygen concentration <u>at</u> the burning surface appears to be around 0.1%-1% (Wooldridge and Muzzy (reference 8), Kulgein (reference 9), Fennimore and Jones (reference 10). This measured non-zero concentration is significant, because earlier JPL work under FAA sponsorship (reference 4) indicated that actual aircraft interior materials exhibited a strong dependence of the kinetics constants of degradation on small concentrations of oxygen in a stream of oxygen in an inert. When it is realized that turbulent transport offers a mechanism for the availability of small concentrations of oxygen at the burning surface, it is easy to see that these oxygen concentration effects could be important in predicting full-scale burning behavior. Full-scale diffusion flames would be large enough to be fully turbulent.

Nevertheless, all the present TG experiments are performed in pure nitrogen except for seat cover fabric, due to the limited scope of the work.

The TG diagrams of the cover fabric, fire blocking layers (Vonar®, LS-200, and Preox®), and foams (polyurethane and polyimide) are shown in figures 4, 5, and 6, respectively. The Arrhenius plots of figures 7, 8, and 9 show that the pyrolysis of each of these materials cannot be described as a single first-order reaction. Thus, the entire reaction temperature range is subdivided into multiple segments in each of which the reaction rate is reasonably accurately described by the first-order Arrhenius expression. Figure 7 shows how it is done for the cover fabric, as an example, with six subdivided segments. Each segment comprises one thermochemical layer as discussed in the previous section.

Kinetics constants obtained along with other thermal and physical data of the materials used in this study are shown in Table I. These are used as input data for the computer program shown in Appendix B.

(b) Burning Tests

In order to measure the temperature profile and weight loss of samples, a modified NBS Smoke Density Chamber is used. The radiative heat flux was provided by a high heat flux furnace (Mellen furnace Model No. 10, with the maximum heat flux of 12 W/cm^2 or 10.6 BTU/ft^2 sec). The originally equipped furnace for the NBS chamber could provide 2.5 W/cm^2. For the temperature distribution measurement, nine thermocouples (Pt vs. Pt-10% Rh) were connected to a multichannel recorder (Leeds and Northrup's Speedomax Model 251, 12 channel, with resolution time of 1 second for each reading). The weight measuring device was a transducer-type cantilever beam, connected to an amplifier and then to a strip-chart recorder.

The furnace is heated up to, and maintained at, 850°C during the tests. After the furnace has reached a steady state, a radiation shield is removed and the seat cushion is exposed directly to the furnace. The radiative heat flux is around ~ 1.6 Btu/ft^2 sec.

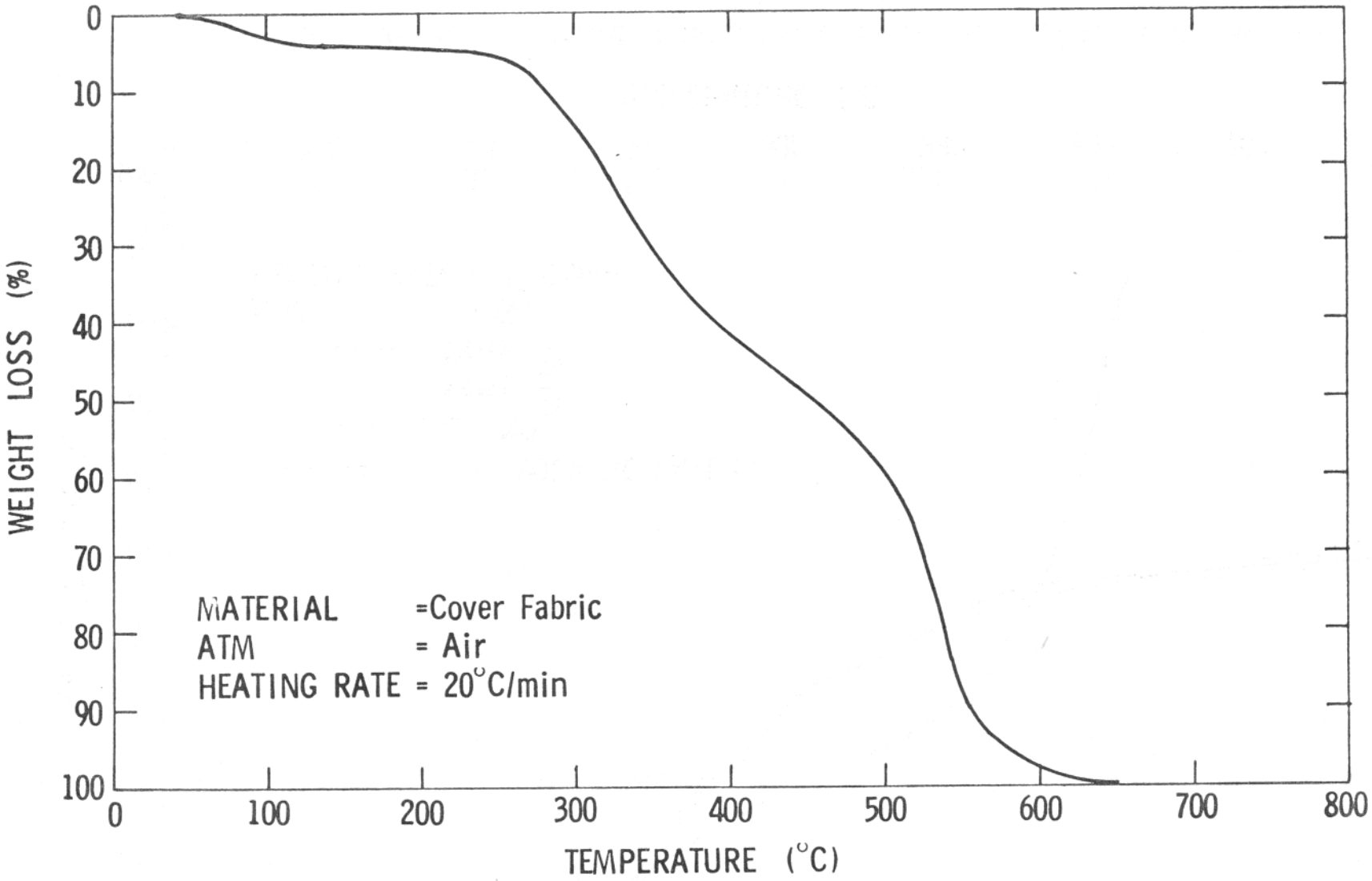

FIGURE 4. THERMOGRAVIMETRIC DIAGRAM OF SEAT CUSHION COVER FABRIC.

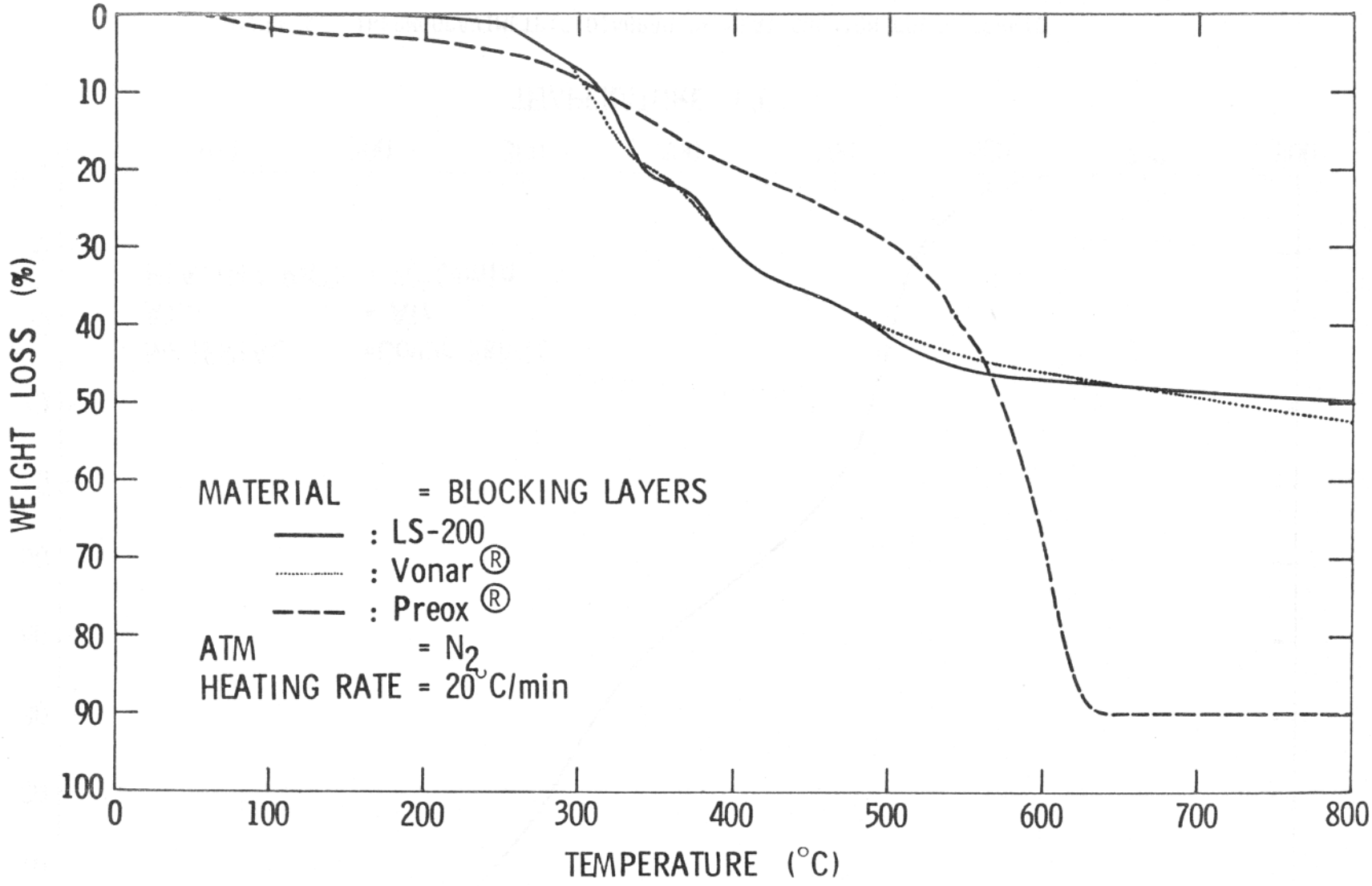

FIGURE 5. THERMOGRAVIMETRIC DIAGRAMS OF THREE FIRE BLOCKING LAYERS, LS-200, VONAR, AND PREOX.

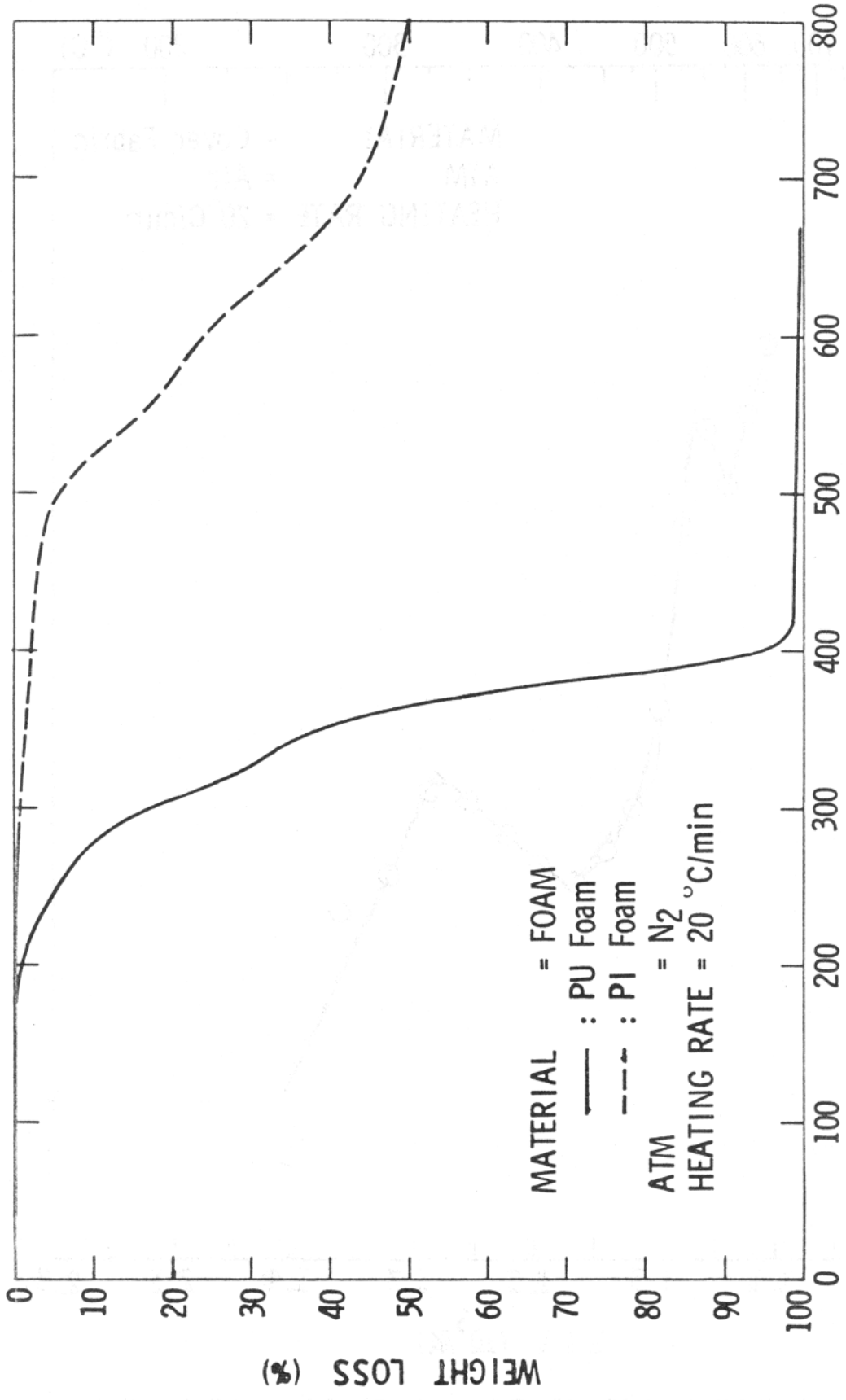

FIGURE 6. THERMOGRAVIMETRIC DIAGRAMS OF TWO FOAMS, POLYURETHANE FOAM AND POLYIMIDE FOAM.

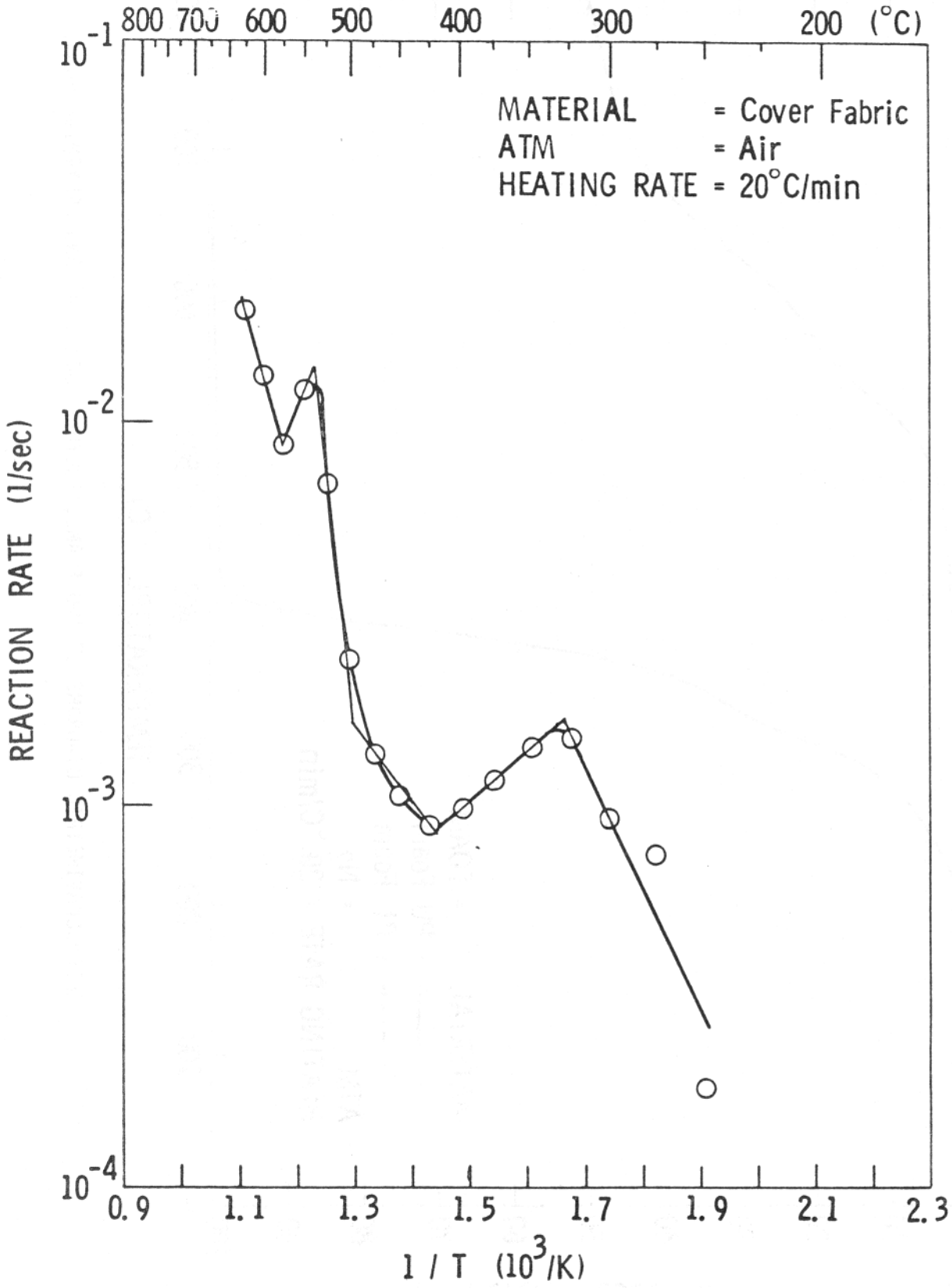

FIGURE 7. ARRHENIUS PLOT OF SEAT CUSHION COVER FABRIC, DEDUCED FROM TG SHOWN IN FIGURE 4.

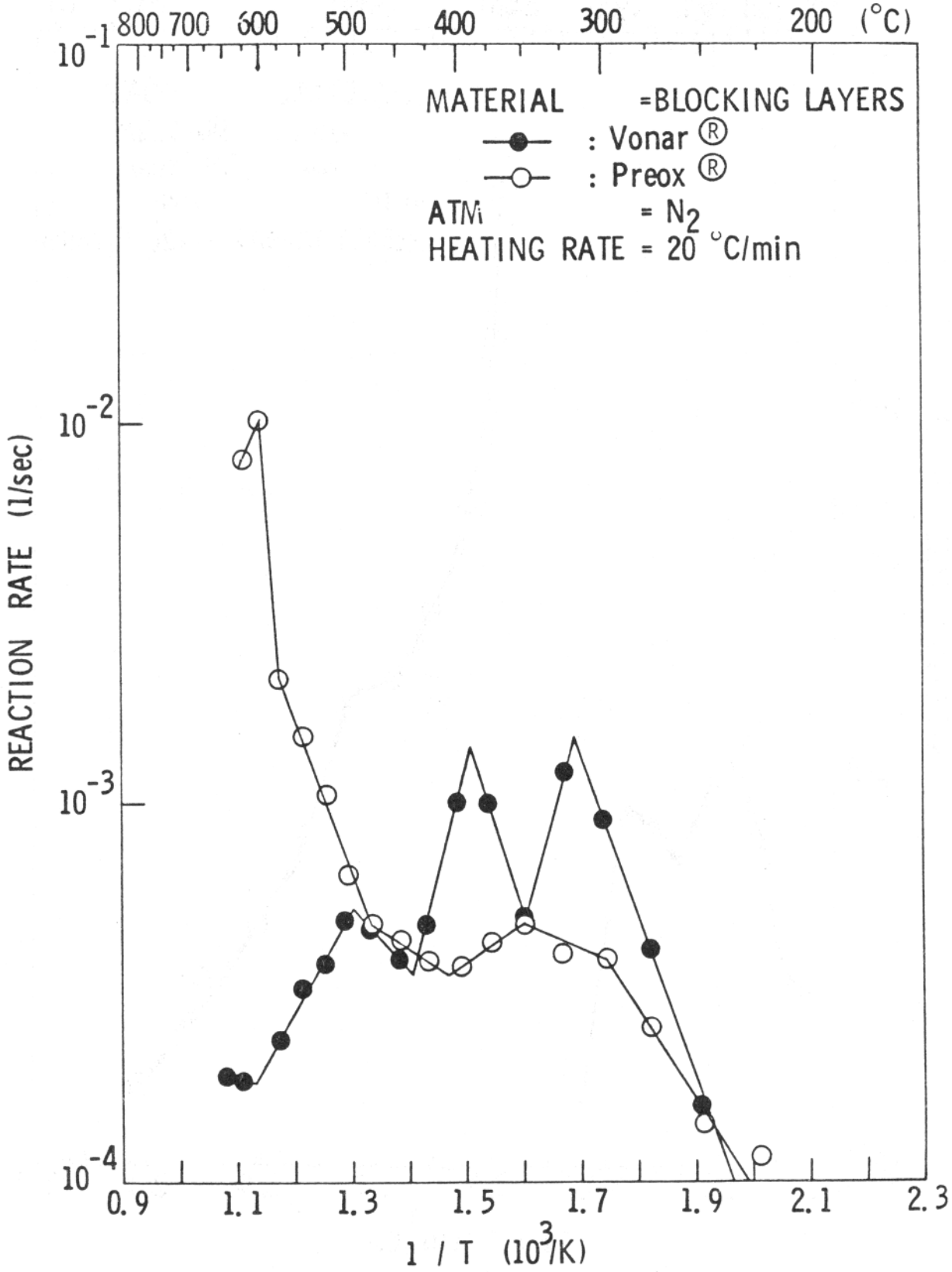

FIGURE 8. ARRHENIUS PLOTS OF TWO FIRE BLOCKING LAYERS, VONAR AND PREOX, DEDUCED FROM TG SHOWN IN FIGURE 5.

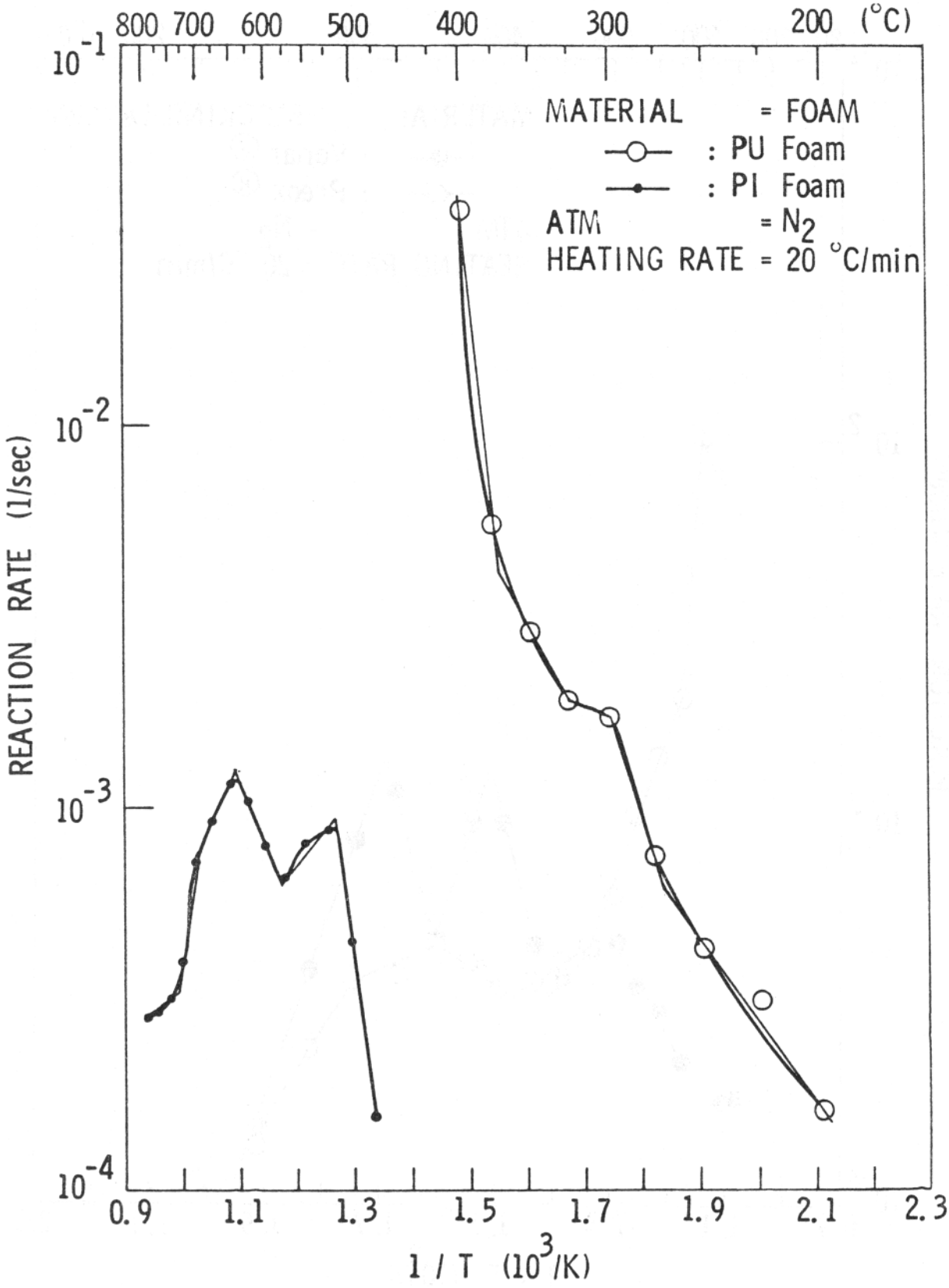

FIGURE 9. ARRHENIUS PLOTS OF POLYURETHANE FOAM AND POLYIMIDE FOAM, DEDUCED FROM TG SHOWN IN FIGURE 6.

Table I(a). Fundamental Properties of Seat Cushion Component Material

	Density $\frac{g}{cm^3}$	c Specific Heat $\frac{cal}{g.°C}$	k* Thermal Conductivity $\frac{cal}{cm.\ sec.°C}$	X_L Thickness cm
Seat Cover Fabric	0.4	0.3	0.0001	0.1
Fire Blocking Layer				
LS-200	0.12	0.3	0.0002	1.2
Vonar®	0.146	0.345	0.0002	0.8
Preox®	0.62	0.3	0.00034	0.1
Foam				
Polyurethane	0.03	0.4	0.00010~0.00034	10.6
Polyimide	0.023	0.2	0.0001	-

(b) Kinetics Constants and Heat of Degradation of Subdivided Thermochemical Layers

	T Temperature Range (K)	B Pre Exponential Factor (1/sec)	E Activation Energy (cal/mole)	D Heat of Degradation (cal/g)
Seat Cover Fabric	848-898	2.13×10^{4}	24800	-2.9
	813-848	5.06×10^{-8}	-20300	-2.9
	763-813	2.24×10^{13}	56500	-2.9
	689-763	2.51×10^{-1}	7800	-2.3
	602-689	7.30×10^{-6}	-6500	-16.
	523-602	1.57×10^{2}	13700	-16.3

* Source: NASA Ames Research Center -- Handbook of Chemistry and Physics

(b) Kinetics Constants and Heat of Degradation of Subdivided Thermochemical Layers (Cont'd)

	T Temperature Range (K)	B Pre Exponential Factor (1/sec)	E Activation Energy (cal/mole)	D Heat of Degradation (cal/g)
LS-200	877-923	1.17×10^{-5}	-3857	0.5
	767-877	7.17×10^{-11}	-24770	9.6
	723-767	5.17×10^{1}	16818	-8.4
	698-723	1.04×10^{-4}	-2020	-19.1
	673-698	8.28×10^{-14}	-31083	-16.7
	648-673	6.56×10^{-3}	2475	-8.4
	623-648	2.46×10^{6}	27897	-20.3
	598-623	1.61×10^{-17}	-38190	7.9
	573-598	2.11×10^{7}	27800	71.9
	548-573	2.01×10^{-1}	6772	24.9
	473-548	7.83×10^{3}	18279	54.9
Vonar®	881-923	3.37×10^{-4}	1043	1.0
	766-881	1.66×10^{-7}	-12285	9.6
	709-766	8.94×10^{-2}	7800	-23.9
	661-709	2.37×10^{-12}	-26532	-28.7
	623-661	2.75×10^{4}	22078	-28.7
	591-623	3.94×10^{-13}	-25933	50.9
	473-591	2.33×10^{4}	19435	107.5
Preox®	873-908	5.42×10^{-6}	-13061	0.5
	848-873	8.55×10^{20}	91578	0.5
	748-848	1.55×10^{2}	18860	0.5
	683-748	9.85×10^{-3}	4500	-13.9
	623-683	1.43×10^{-5}	-4365	-13.9
	573-623	5.87×10^{-3}	3085	-13.9
	498-573	5.94×10^{0}	10963	0.5
Polyurethane Foam	644-688	8.44×10^{19}	65760	3.1
	598-644	6.17×10^{1}	12335	11.9
	573-598	1.77×10^{-2}	2646	2.5
	544-573	2.60×10^{5}	21435	2.5
	448-544	6.00×10^{0}	9900	0.5
Polyimide Foam	1006-1073	3.06×10^{-5}	-4763	0.5
	973-1006	3.12×10^{-14}	-46170	0.5
	915-973	1.80×10^{-7}	-16070	0.5
	854-915	1.33×10^{1}	16860	-7.3
	796-854	6.11×10^{-6}	-7890	-7.3
	711-796	1.07×10^{7}	36705	-7.0
	673-711	7.63×10^{-3}	6938	-0.3

(c) A Note on the Heating Rates

The actual heat fluxes encountered in aircraft crash situations can approach 10 W/cm^2 -- a fact that led investigators to recognize that the NBS smoke-density chamber, with its original 2.5 W/m^2 furnace, may have to be modified for realistic simulations. In the present effort, the heat fluxes meant for the FAA samples were planned to be gradually increased from a low value (1 W/cm^2) to the full value of 6-10 W/cm^2. It was the plan to verify the model at low heat fluxes first in a logical sequence of increasing heat fluxes. Thus, at the time of the present reporting the lower heat fluxes have been investigated. The capability exists for the higher heat fluxes. However, the actual tests await future research support.

Since the initial setup of equipment and trial runs, several modifications and improvements have been made on the sample preparation and run procedure, in order to obtain meaningful and reproducible test results. These are listed in appendix C for future reference.

A pair of thermocouples are placed at every interface, including the front surface. And additional five are placed within the polyurethane foam, 0.5 inches apart from each other along the axis. A test is always run in duplicate; one to measure the weight loss and the other for the temperature profile. This is because the thermocouples have such stiffness that their use would not allow free movement of the cantilever beam and the accurate measurement of weight change.

4. RESULTS AND DISCUSSION

(a) Burning Test Results

The pictures of the burned samples and the equipment used in this work are shown in appendix D for visual examination. The results of the burning tests in the modified NBS Smoke Density Chamber are

shown in figure 10. These are the temperature changes obtained from the multiple thermocouple readings placed at different positions within the seat cushion assemblies and the weight change with time, for the runs with and without the fire blocking layers.

The weight change data show that the sample without a fire blocking layer suffered the largest mass loss, and that the effectiveness of a fire blocking layer, if judged from the mass loss data, can be rated in increasing effectiveness on Preox®, Vonar®, and LS-200. The same order is observed when the burnt samples were examined visually.

The thermocouple reading at the sample surface facing the furnace, however, should be corrected for the caused by radiation and convection. The energy balance for the thermocouple bead can be shown as

$$h_{rad} (T_{furnace} - T_{bead}) = h_{conv} (T_{bead} - T_{gas\ film})$$

where h_{rad} and h_{conv} are the radiative and convective heat transfer coefficient, respectively, and $T_{furnace}$, T_{bead}, $T_{gas\ film}$ are the temperatures of the furnace, thermocouple bead, and film stagnant gas film surrounding the bead, respectively. The estimated error ($T_{actual} - T_{bead}$) is in the range of 25°C to 35°C under the current experimental conditions. Further detailed error analysis is not attempted here due to the lack of precise information on emittance, sample surface condition, and thermal contact between the bead and fabric fibers, which are necessary to estimate the heat transfer coefficients with sufficient precision.

Other than this, the thermocouple data lead to a few important observations.

(1) The first one is that the front surface temperature measured by the thermocouple No. 1 reaches a steady state in about three

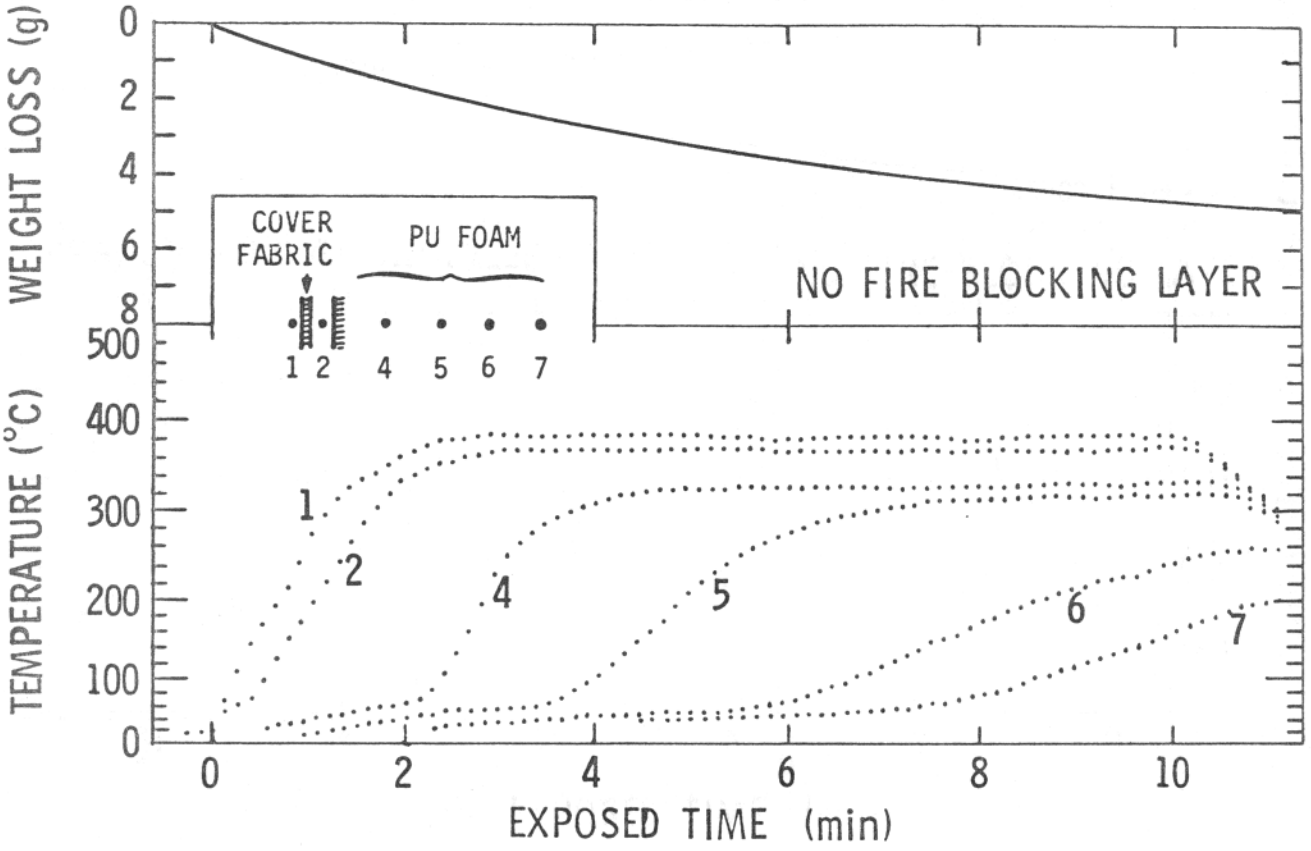

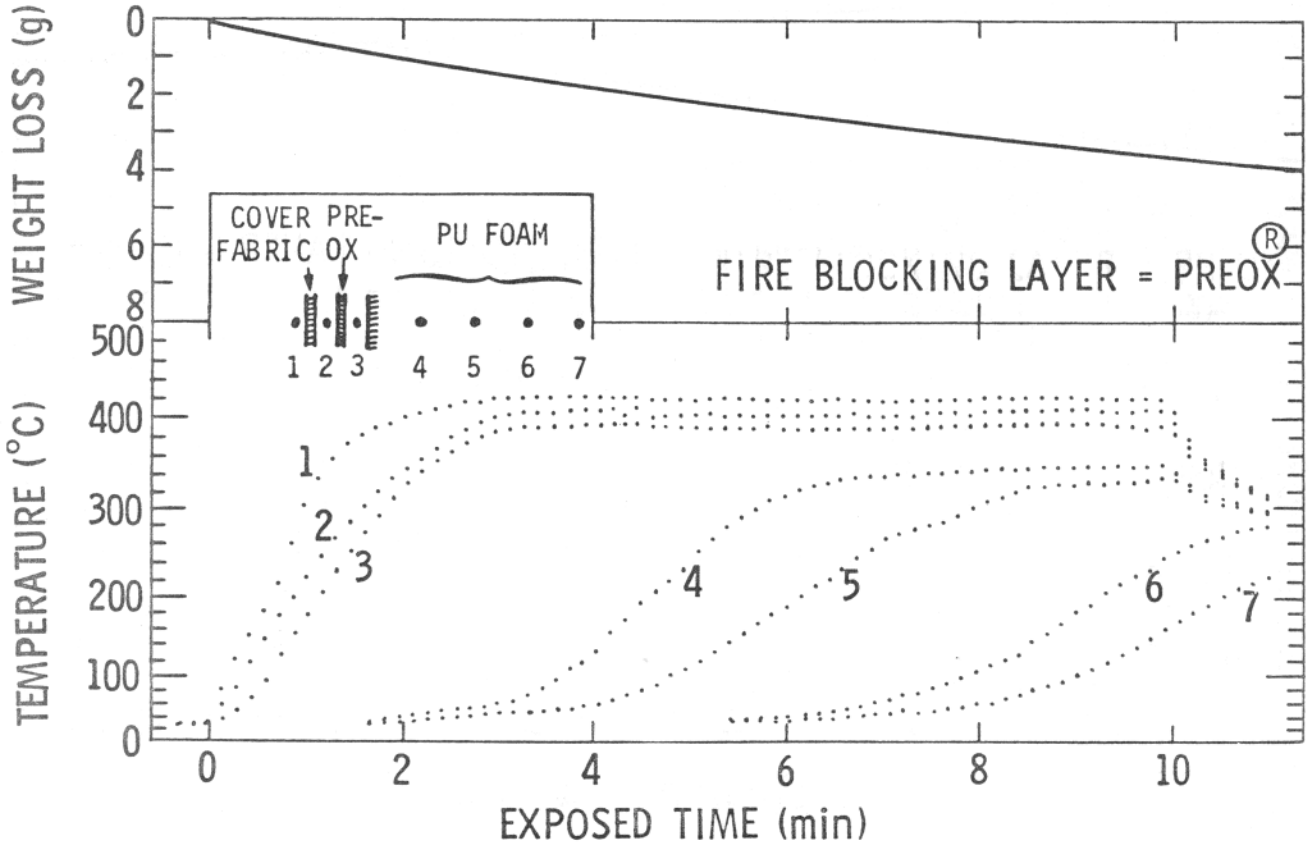

FIGURE 10. WEIGHT AND TEMPERATURE CHANGE DATA MEASURED DURING THE BURN TESTS IN A MODIFIED NBS SMOKE CHAMBER WITH AND WITHOUT A FIRE BLOCKING LAYER. (1 of 2 pages)

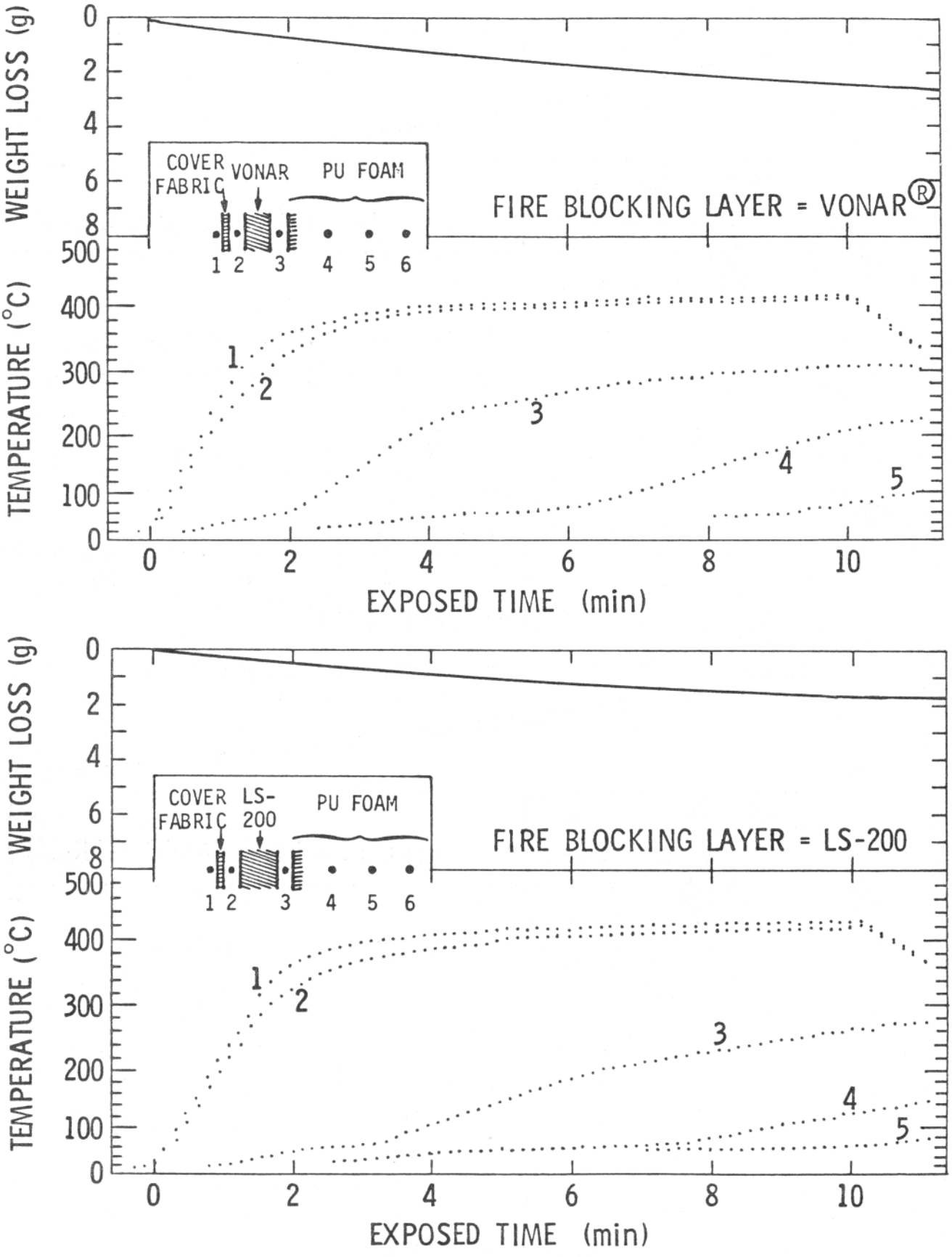

FIGURE 10.

FIGURE 10. WEIGHT AND TEMPERATURE CHANGE DATA MEASURED DURING THE BURN TESTS IN A MODIFIED NBS SMOKE CHAMBER WITH AND WITHOUT A FIRE BLOCKING LAYER (2 of 2 pages)

minutes, and then registers essentially the same temperature thereafter. When a fire blocking layer of Vonar® or LS-200 is used, however, a very slight increase of the front surface temperature is observed. The temperature just behind the cover fabric, measured by the thermocouple No. 2, trails that of the front surface by about 15°C.

(2) There is a further temperature drop across a fire blocking layer. This temperature drop is indicated by the vertical distance between the thermocouples No. 2 and No. 3 readings, as shown in figure 10. In the figure, LS-200 allows the largest temperature drop, Vonar® medium, and Preox® the least. Incidentally this is exactly the opposite order as the one observed in total mass loss.

(3) The temperature-rise histories within the polyurethane foam, measured by thermocouples No. 4, 5, 6, and 7, hardly represent steady-states. Most of the measured temperatures simply keep rising steadily, as shown in figure 10.

In some cases, however, a plateau seems to appear after such monotonic increase in temperature, implying a steady-state condition attained within the foam. This behavior is believed to be caused by the formation and existence of a void or dome filled with relatively hot pyrolysis gas products in a convective flow motion. This explains why such a plateau shows up and why then these plateaus are close to each other - in other words, the temperature gradient is small. It is particularly serious when no fire blocking layer is used, because under the condition of high heat flux, the polyurethane foam liquefies and drips before complete burnout occurs. This eventually leaves an ever-growing void filled with the hot pyrolysis gas product. The hot gas of the void may flow freely and contribute to the rapid temperature rise at the rear surface.

(4) The use of a fire blocking layer helps maintain lower temperatures at the rear (colder) side essentially by reducing the heat transfer. This can be seen easily by comparing the temperatures measured by the thermocouples with the same number. For example, after 6 minutes of exposure, the thermocouple No. 5 reaches 321 K with LS-200, 323 K with Vonar®, and 463 K with Preox®, while it reaches 546 K without a fire blocking layer.

There is, however, a compensating effect near the front (hot) surface. That is, the front attains higher temperatures with the fire blocking layer than would be observed without the fire blocking layer. Figure 10 shows the front surface temperature is 701 K with LS-200, 695 K with Vonar®, 691 K with Preox®, and 643 K without one, respectively, after 10 minutes exposure. This leads to an observation that a fire blocking layer functions as if it is a reflector for heat flux.

This results in lowering the rear side temperature while maintaining the higher front side temperature.

(b) Predictions by Thermochemical Model

The temperature profiles obtained by the thermochemical model, in comparison with the experimental data, are shown in figure 11. The profile for each configuration (with and without a fire blocking layer) is calculated every 2 minutes using the Computer Program B of appendix B. (Note: The conductive heat flux at the front surface, needed as the input for the Computer Program B, was the one predicted by Computer Program A of appendix B.) In general, the calculated results are in good agreement with the experimental data. The difference is often less than 10°C, with a few exceptions of 25°C as the maximum difference. However, the predicted temperatures within the polyurethane foam show significant deviations from the measurements. The negative deviations, i.e., temperatures measured lower than predicted, are seen when the exposed time is small and/or

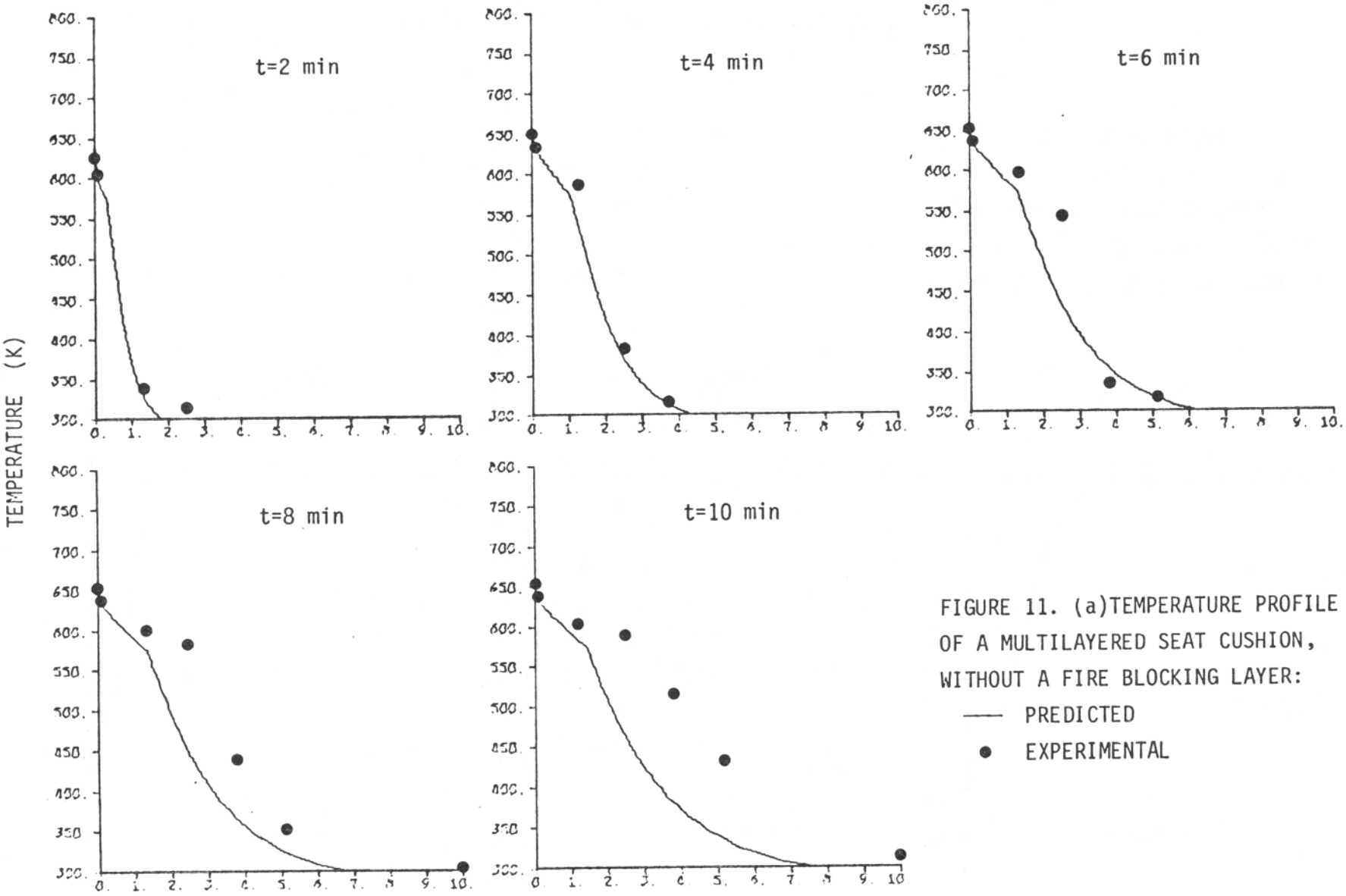

FIGURE 11(a)

FIGURE 11. (a)TEMPERATURE PROFILE OF A MULTILAYERED SEAT CUSHION, WITHOUT A FIRE BLOCKING LAYER:

—— PREDICTED

● EXPERIMENTAL

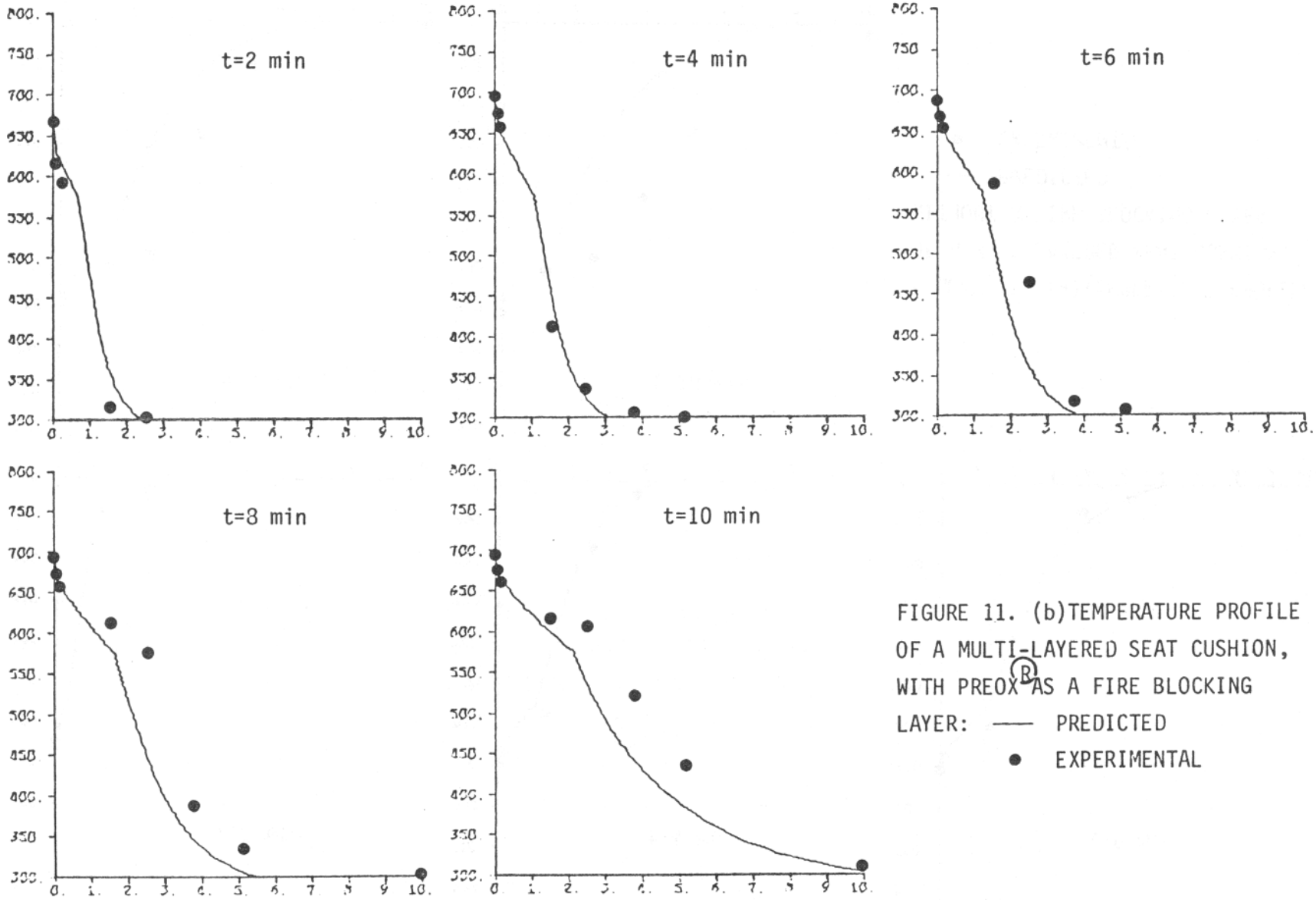

FIGURE 11(b)

FIGURE 11. (b)TEMPERATURE PROFILE OF A MULTI-LAYERED SEAT CUSHION, WITH PREOX® AS A FIRE BLOCKING LAYER: —— PREDICTED
● EXPERIMENTAL

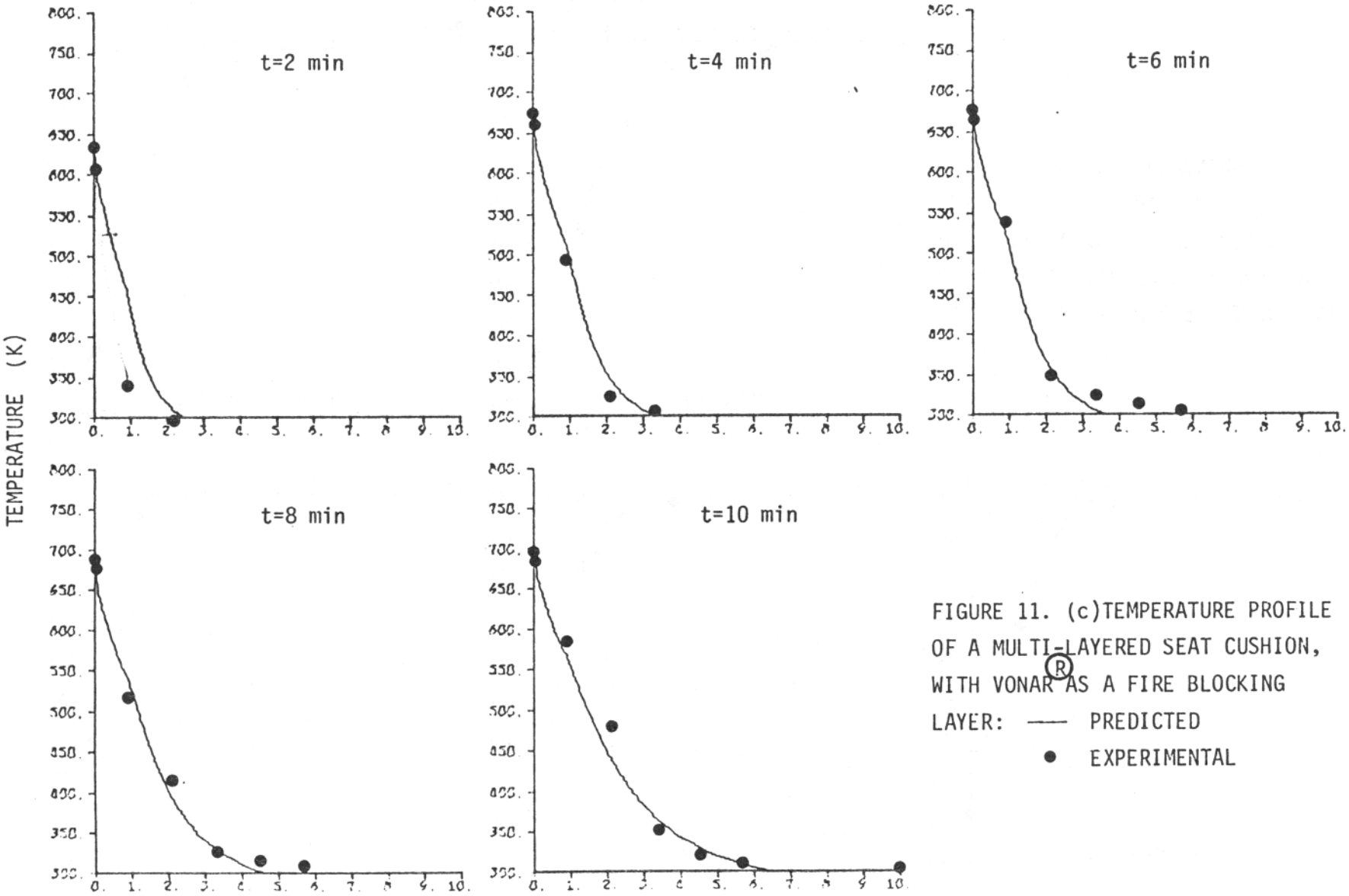

FIGURE 11(c)

FIGURE 11. (c)TEMPERATURE PROFILE OF A MULTI-LAYERED SEAT CUSHION, WITH VONAR® AS A FIRE BLOCKING LAYER: —— PREDICTED
● EXPERIMENTAL

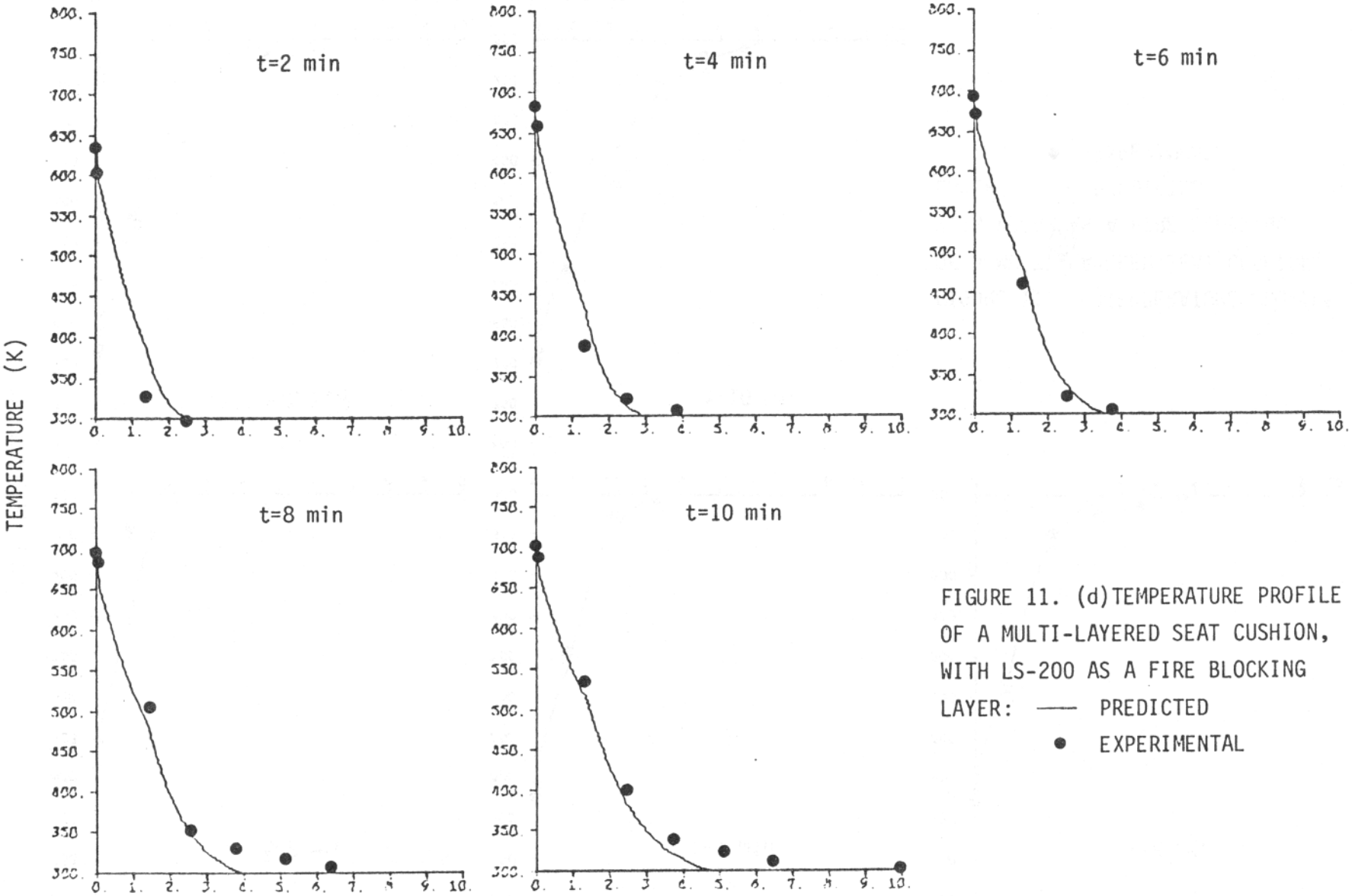

FIGURE 11(d)

FIGURE 11. (d) TEMPERATURE PROFILE OF A MULTI-LAYERED SEAT CUSHION, WITH LS-200 AS A FIRE BLOCKING LAYER: —— PREDICTED
● EXPERIMENTAL

where the depth is large. The positive deviations, i.e., temperatures measured higher than predicted, are seen wherever the void is observed inside of the polyurethane foam. This is again believed to be caused by a convective flow of hot combustion gas within the void, which leads to increased heat transfer to the colder side.

The weight losses calculated by the model are compared with the experimental data, as shown in figure 12. The figure shows that the calculated weight loss is about 15 to 95 percent higher than the measured values in all cases, but the order of the mass loss is in agreement with the experimental data except for the control (without a fire blocking layer). This again is due to the presence of the void formed inside of the foam, which is clearly the physical state this thermochemical model is not aimed to be used for.

5. SUMMARY

The work on the prediction of thermochemical performance of multi- layered seat cushion materials leads to four conclusions:

1. The concept of thermochemical sublayers is applicable to describe the complex pyrolysis behavior observed for many of the currently used and proposed aircraft interior polymeric materials.

2. The thermochemical model of the past can be extended to handle such multilayered systems analytically.

3. The model predicts reasonably within a factor of 2 both the weight loss due to burning and the temperature profile established within the seat materials.

4. The thermochemical model, can be used with the minimum number of input data determined by experiments for the thermochemical performance prediction of other multilayered materials under fire conditions. This analysis coupled with experiments in the NBS Smoke Chamber offers a useful small-scale test procedure for evaluating candidate blocking layer materials.

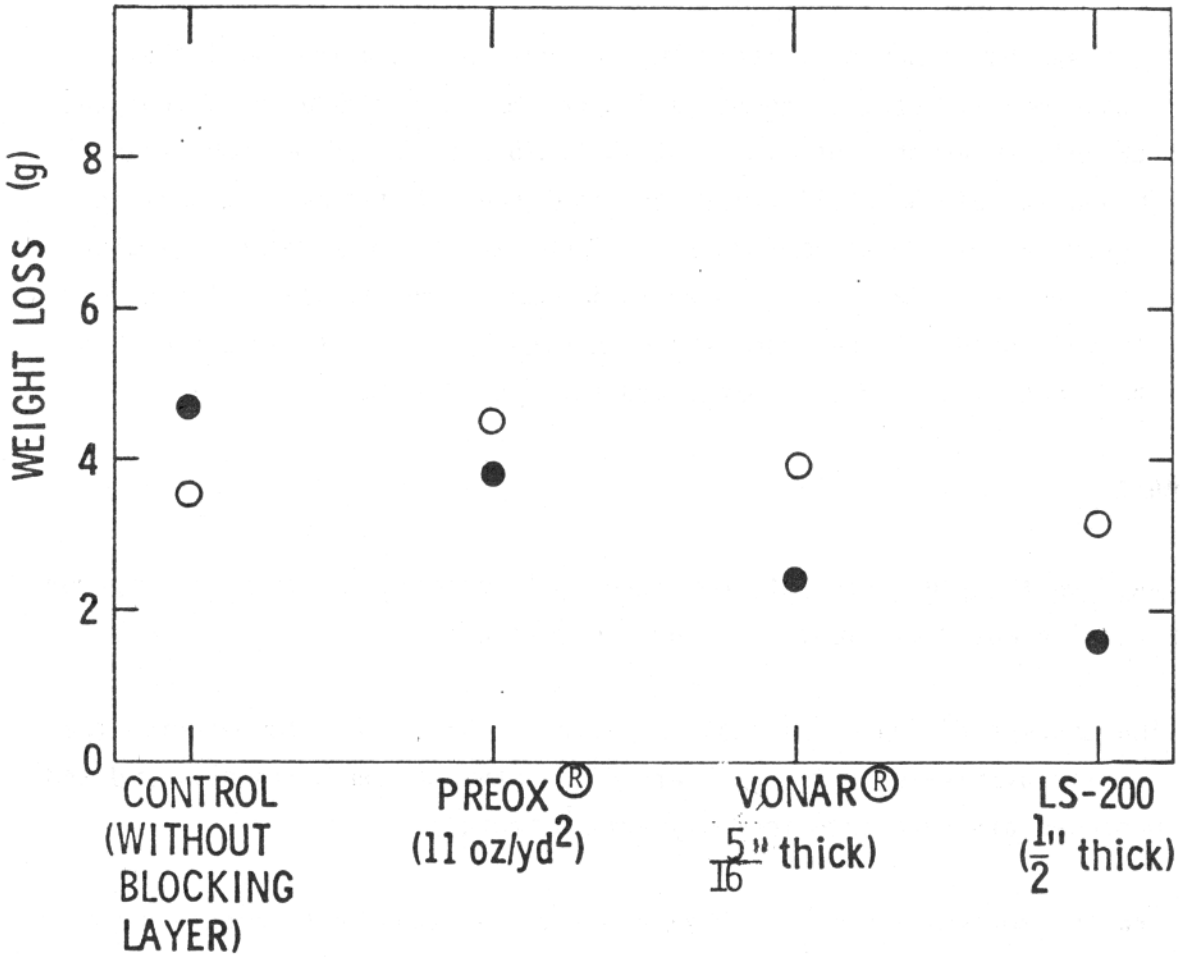

FIGURE 12. COMPARISON OF MASS LOSSES PREDICTED BY THE MODEL AND THE EXPERIMENTAL DATA (AFTER 10 MINUTES OF BURNING IN THE NBS SMOKE CHAMBER): ○ - PREDICTED
● - EXPERIMENTAL

REFERENCES

1. Howell, W., Opening Remarks in Workshop on Mathematical Fire Modeling, March 24-27, 1981, proceedings, Aug. 1981, U. S. Department of Transportation, Federal Aviation Administration, Report No. DOT/FAA/CT-81/209.

2. Sarkos, C., Aircraft Fire Scenarios, ibid.

3. Eklund, T., FAA Modeling Efforts, ibid.

4. Dokko, W. and Ramohalli, K., Application of Thermochemical Modeling to Aircraft Interior Polymeric Materials, U.S. Department of Transportation, Final Report No. DOT/FAA/CT-82/83.

5. Ramohalli, K. and Mink, M., Thermal Performance Modification of Composite Materials, AIAA 17th Aerospace Sciences Meeting, New Orleans, Louisiana, January 1979, Paper No. 79-0018.

6. Kumar, R. N. and Stickler, D. B., Polymer Degradation Theory of Pressure- Sensitive Hybrid Combustion, XIII Symposium (International) on Combustion, The Combustion Institute, 1971, pp. 1059-1072.

7. Kourtides, D. A. and Parker, J. A., Test Methodology for Evaluation of Fireworthy Aircraft Seat Cushions, J. Fire & Flamm., Vol. 15, pp. 56-76, 1982.

8. Woolridge, C.E. and Muzzy, R.J., "Experiments in a Turbulent Boundary-Layer with transpiration on Combustion," X Sumposium (International) in Combustion, The Combustion Institute, 1965, p. 1337.

9. Kulgein, p. 417, JFM 12 (1962).

10. Fennimore, C.P. and Jones, G.W., C&F, X, p. 295 (1966).

11. Spalding, D.B., "Some Fundamentals of Combustion," Butterworth, London, (1954).

APPENDIX A Derivation of r

The differential equations are

$$k \frac{d^2T}{dx^2} + \rho_{cr} \frac{dT}{dx} = D\rho NB \exp(-E/RT) \tag{A-1}$$

$$-\frac{1}{N}\frac{dN}{dt} = B \exp(-E/RT) \tag{A-2}$$

and the boundary conditions are

$$\text{at } x = 0 \qquad T = T_S \tag{A-3}$$

$$N = N_S = 1 - \frac{1}{FS_S}$$

$$\text{at } x = x_L \qquad T = T_C \tag{A-4}$$

$$N = N_C = 1 - \frac{1}{FS_C}$$

By introducing the dimensionless terms,

$$y = \frac{\rho_{cr}\, x}{k} \tag{A-5}$$

and

$$\tau = \frac{T-T_O}{T_S-T_O} \tag{A-6}$$

Then Eqs. (A-1) and (A-2) become

$$\frac{d^2\tau}{dy^2} + \frac{d\tau}{dy} = \frac{kD\rho NB \exp(-E/RT)}{(\rho cr)^2 (T_S-T_O)} \tag{A-7}$$

$$\frac{dN}{d\tau} \cdot \frac{d\tau}{dy} = \frac{k\, c\rho\, NB \exp(-E/RT)}{(\rho cr)^2} \tag{A-8}$$

Further use of dimensionless variables,

$$p = \frac{d\tau}{dy} \tag{A-9}$$

$$h = \frac{D}{c(T_S - T_O)} \tag{A-10}$$

and

$$\Lambda = \frac{kB}{\rho_c r^2} \tag{A-11}$$

convert the Eqs. (A-7) and (A-8) to

$$pp' + p = \Lambda h N \exp(-E/RT) \tag{A-12}$$

$$pN' = \Lambda N \exp(-E/RT) \tag{A-13}$$

where a prime denotes $d/d\tau$.

The boundary conditions are accordingly

$$\tau = 1, \quad p = p_S, \quad N = N_S \tag{A-14}$$

$$\tau = \tau_C, \quad p = p_C, \quad N = N_C \tag{A-15}$$

The Eq. (A-13) can be combined to Eq. (A-12) to yield

$$pp' + p - pN'h = 0 \tag{A-16}$$

Assuming $p \neq 0$, then Eq. (A-16) becomes essentially

$$\frac{dp}{d\tau} + 1 - \frac{dN}{d\tau} = 0 \tag{A-17}$$

If Eq. (A-17) is integrated using the boundary conditions of Eqs. (A-14) and (A-15), then

$$N = (p + \tau - p_S - 1 + h N_S)/h \tag{A-18}$$

$$\text{or} \quad N = (p + \tau - p_C - \tau_C + h N_C)/h \tag{A-19}$$

Then substituting Eq. (A-19) into Eq. (A-12) gives

$$pp' + p = \Lambda(p + \tau - p_s - 1 + h N_s) \exp(-E/RT) \qquad \text{(A-20)}$$

This is the differential equation to be solved with the boundary equations (A-14) and (A-15).

If the T is close to T_s, then as an approximation, Eq. (A-20) can be written as

$$pp' + p = (p + \tau - p_s - 1 + h N_s) \Lambda \exp\left\{ -\Theta [1 + \chi(1-\tau)] \right\} \qquad \text{(A-21)}$$

where $$\Theta = \frac{E}{RT_s}, \qquad \text{(A-22)}$$

and $$\chi = \frac{T_s - T_o}{T_s} \qquad \text{(A-23)}$$

Let $$\lambda\!\!\!^{-} = \Lambda \exp(-\Theta) \qquad \text{(A-24)}$$

and $$g = -p_s - 1 + hN_s \qquad \text{(A-25)}$$

then, the Eq. (A-21) is

$$pp' + p = (p + \tau + g)\ \lambda\!\!\!^{-} \exp[-\Theta \chi(1-\tau)] \qquad \text{(A-26)}$$

Further defining

$$\eta = \frac{1-\tau}{\varepsilon} \qquad \text{(A-27)}$$

$$\xi = p + \tau \qquad \text{(A-28)}$$

$$\lambda = \varepsilon \lambda\!\!\!^{-} \qquad \text{(A-29)}$$

where $$\varepsilon = \frac{1}{\Theta\chi} \qquad \text{(A-30)}$$

enables rewriting Eq. (A-26) as

$$-(\xi - 1 + \varepsilon\eta)\,\xi' = (\xi + g)\,\lambda \exp(-\eta) \tag{A-31}$$

or

$$\frac{d\xi}{\xi + g} - \frac{\xi d\xi}{\xi + g} = \lambda e^{-\eta}\, d\eta \tag{A-32}$$

The boundary conditions for this equation are

$$\eta = 0 \quad \xi = \xi_s = p_s + 1 \tag{A-33}$$

$$\eta = \eta_c \quad \xi = \xi_c = p_c + \tau_c \tag{A-34}$$

Integrating now with respect to ξ and η, in the region between two surfaces, s and c, is

$$\int_c^s \frac{d\xi}{\xi + g} - \int_c^s \left(\frac{\xi}{\xi + g}\right) d\xi = \int_c^s \lambda e^{-\eta} d\eta \tag{A-35}$$

to give the result as

$$\ln\left(\frac{\xi_s + g}{\xi_c + g}\right) - \left\{(\xi_s - \xi_c) - g \ln\left(\frac{\xi_s + g}{\xi_c + g}\right)\right\} = -\lambda(1 - e^{-\eta_c}) \tag{A-36}$$

Then λ is simply given by

$$\lambda = \frac{1}{(1 - e^{-\eta_c})} \cdot \left\{(\xi_s - \xi_c) + (1 + g) \ln\left(\frac{\xi_c + g}{\xi_s + g}\right)\right\} \tag{A-37}$$

By combining Eq. (A-29), (A-30), (A-22), (A-23) and (A-11), r can be shown in more familiar terms,

$$r = \sqrt{\frac{(k/\rho c)\, B \exp(-E/RT_s)}{\lambda \left(\frac{E}{RT_s}\right)\left(\frac{T_s - T_0}{T_s}\right)}} \tag{A-38}$$

APPENDIX B Computer Program

```
1*      C                                  PROGRAM A
2*      C  THIS PROGRAM TAKES THE INTERFACIAL TEMPERATURES (B.C.'S) AS THE INPUT
3*      C  DATA AND THEN CALCULATES THE BURNING RATE, HEAT FLUX, TEMPERATURE PROFIL
4*      C  AND WEIGHT LOSS OF MULTI-LAYERED POLYMERIC MATERIALS (INCLUDING
5*      C  THE FIRE BLOCKING LAYER) USED FOR AIRCRAFT SEAT CUSHIONS.
6*      C  THE DIMENSIONS USED IN THIS PROGRAM ARE GRAM, GRAM-MOLE, D-CELSIUS,
7*      C  CALORIE, CM, AND SECOND.
8*      C
9*            DIMENSION ANAMET(7,2),MW(7),NTREG(7),KT(7,11),CPT(7,11),
10*           -  RHOT(7,11),BT(7,11),ET(7,11),DT(7,11),HEATRT(7,11),
11*           -  TKLO(7,11),TKHI(7,11),TLO(11),THI(11),
12*           -  EKLO(7,11),EKHI(7,11),ELO(11),EHI(11),
13*           -  NKLO(7,11),NKHI(7,11),NLO(11),NHI(11),
14*           -  JSTART(11),JEND(11),HEADIN(14),ID(11),
15*           -  NS(11),NC(11),ANAME(11,2),T(11),K(11),CP(11),RHO(11),B(11),
16*           -  E(11),D(11),HEATRA(11),ESS(11),ESC(11),RB(11),GIN(11),GOUT(11),
17*           -  QNET(11), TP(11,11),NSSP(11,11),TSTART(11),TINTV(11)
18*            DIMENSION TPLOT(121),YPLOT(121),RHS(11,11),DXDT(11,11),DY(11,11)
19*            DIMENSION X(11,11)
20*            DIMENSION W(11),PS(11),PC(11),YIS(11),YIC(11),THETA(11),ETAC(11)
21*            DIMENSION ENC(11),LAMBDA(11),CHI(11),ALPHA(11)
22*            DIMENSION TIC(11),RORC(11),A(11),G(11),RBT(11)
23*            REAL KT,K,MW,NS,NC,NKLO,NKHI,NLO,NHI,LAMBDA
24*     C
25*     C  READ IN THE INGREDIENT MATERIAL PROPERTY AND PRINT OUT
26*     C
27*            READ (5,901) ITOTAL
28*       901  FORMAT (I2)
29*            DO 100  II=1,ITOTAL
30*                  READ (5,902) I,ANAMET(I,1),ANAMET(I,2),MW(I),NTREG(I)
31*       902        FORMAT(I2,2A5,F10.2,I2)
32*                  NTR=NTREG(I)
33*                  READ (5,903)(TKLO(I,J),TKHI(I,J),KT(I,J),CPT(I,J),RHOT(I,J),
34*              -                  BT(I,J),ET(I,J),DT(I,J),HEATRT(I,J),J=1,NTR)
35*       903        FORMAT (2F5.1, 7E10.3)
36*       100  CONTINUE
37*            WRITE (6,948)
38*       948  FORMAT (1H1, 25X, 'BURNING RATE PREDICTION FOR MULTI-LAYERED'
```

```
*           - ' AIRCRAFT SEAT CUSHION' / 26X, 63('='), /
*           -      5X, 'MATERIAL PROPERTY'/  21X, 'TEMP. RANGE.    THERMAL', 5X,
*           - 'HEAT', 6X,'DENSITY     PREEXP.     ACTIVATION    HEAT OF     HEAT',
*           - 5X      / 36X, 'CONDUCTIV.  CAPACITY',13X, 'FACTOR      ENERGY',
*           - 7X, 'DECOMPOS.  RATE', /
*           -26X, '(K)', 5X,'(CAL/CM.S.C)  (CAL/GM.C) (GM/CM3)', 13X,
*           -'(CAL/MOLE)    (CAL/GM)    (DEG C/SEC)'  /)
*            DO 102 I=1,ITOTAL
*            NTR=NTREG(I)
*            WRITE (6,951)  I,ANAMET(I,1),ANAMET(I,2)
*       951 FORMAT (5X,I2,2X,2A5)
*            WRITE (6,953) (TKLO(I,J),TKHI(I,J),
*           -  KT(I,J),CPT(I,J),RHOT(I,J),PT(I,J),ET(I,J),DT(I,J),HEATRT(I,J),
*           -       J=1,NTR)
*       953 FORMAT (17X, F7.1, '-', F7.1, 1X,
*           -       F10.5,3X, F6.3, 3X, F6.3, 2X, E11.3, 4X, F9.0, F10.1, F10.2)
*       102 CONTINUE
      C
      C  FIX CONSTANTS USED IN THIS PROGRAM
      C
            P=1.0
            R=1.98717
            PM=82.06
            CPGAS=0.382
            EPSLON=0.9
            SIGMA=1.355E-12
            TO=225.0
      C
      C  CALCULATE N AND FS  AT TWO END TEMPERATURES OF KINETIC REGIMES
      C  THE CALCULATION SEQUENCE IS, BY LOGIC, FROM LOW TO HIGH TEMPERATURE
      C
            WRITE (6,955)
       955 FORMAT (1H1, 10X, 'NORMALIZED FRAGMENT SIZE AT END TEMPS OF', 1X,
           - 'KINETIC REGIMES', /, 11X, 56('='), /)
            DO 200 I=1,ITOTAL
                  WRITE (6,951) I, ANAMET(I, 1), ANAMET(I,2)
                  NTR=NTREG(I)
                  NKLO(I,NTR)=1.0
                  FKLO(I,NTR)=10000.
            DO 205 JJ=1,NTR
               J=NTR+1-JJ
                  CALL FRAGMT (RT(I,J),ET(I,J),TKLO(I,J),TKHI(I,J),
           -            HEATRT(I,J),NKLO(I,J),NKHI(I,J))
                  IF (J.NE.1) NKLO(I,J-1)=NKHI(I,J)
                  IF (NKLO(I,J).EQ.1.0) NKLO(I,J)=0.9999599
                  FKLO(I,J) = 1.0/(1.0-NKLO(I,J))
                  IF (NKHI(I,J).EQ.1.0) NKHI(I,J)=0.9999599
                  FKHI(I,J) = 1.0/(1.0-NKHI(I,J))
                  WRITE (6,958) TKLO(I,J),TKHI(I,J),NKLO(I,J),NKHI(I,J)
       958 FORMAT (22X, F7.1, '-', F7.1, 5X, F11.6, 2X, '--', 1X, F11.6)
       205 CONTINUE
       200 CONTINUE
      C
      C  INITIALLIZE A FEW VARIABLES FOR COMPUTER PLOTTING
      C
            NPAGE=9
            NPLOT=1
```

```
      IPLOT=0
      CALL BGNPLT
C
C  READ IN TEMPERATURE DATA, I.E.,
C  TEMP. OF TOP SURFACE OF EACH LAYER AND REAR SURFACE (COLD)
C
 1111 CONTINUE
      WRITE (6,898)
  898 FORMAT (1H1, 25X, *BURNING RATE PREDICTION FOR MULTI-LAYERED*
     - * AIRCRAFT SEAT CUSHION* / 26X, 63(*=*), /)
      READ (5,904,END=1112) TBACK,(HEADIN(I),I=1,14)
  904 FORMAT (F10.0,14A5)
      WRITE (6,899) (HEADIN(I),I=1,14)
  899 FORMAT (40X, 14A5, ///
     -     5X, *MATERIAL *              7X, *SURFACE   THERMAL      HEAT
     -   DENSITY    PREEXP.     ACTIVATION   HEAT OF     HEAT          *,/
     -21X, *TEMP.      CONDUCTIV.  CAPACITY               FACTOR      ENERGY
     -        DECOMPOS.  RATE*,/
     -21X, *(K)*, 5X,*(CAL/CM.S.C)  (CAL/GM.C) (GM/CM3)*, 13X,
     -*(CAL/MOLE)   (CAL/GM)   (DEG C/SEC)* ///)
      I=1
  105 CONTINUE
      READ (5,906,END=110) ID(I),THI(I)
  906 FORMAT (I2,F10.2)
      I=I+1
      GO TO 105
  110 CONTINUE
      NLAYG=I-1
C
      NLAYG1=NLAYG-1
      DO 115 I=1,NLAYG1
  115 TLO(I)=THI(I+1)
      TLO(NLAYG)=TBACK
C
C  NOW CALCULATE THE FRAGMENT SIZES AT THE TWO BOUNDARIES OF EACH
C  GENERIC LAYER
C
      DO 300 I=1,NLAYG
      IDENT=ID(I)
      NTID=NTREC(IDENT)
      IF (TLO(I).GE.TKLO(IDENT,NTID)) GO TO 301
      JSTART(I)=NTID
      NLO(I)=1.0
      FLO(I)=10000.
      GO TO 304
  301 CONTINUE
            DO 302 J=1,NTID
            IF (TLO(I).GE.TKLO(IDENT,J).AND.TLO(I).LT.TKHI(IDENT,J))
     -                  GO TO 305
  302       CONTINUE
            WRITE (6,961) I
  961       FORMAT (5X,*FOR *, I2, *TH LAYER, TLO IS OUT OF BOUND*)
            GO TO 304
  305       JSTART(I)=J
            CALL FRAGMT(BT(IDENT,J),ET(IDENT,J),TKLO(IDENT,J),TLO(I),
     -           HEATRT(IDENT,J),NKLO(IDENT,J),NLO(I))
            FLO(I) = 1.0/(1.0-NLO(I))
```

```
      304 CONTINUE
          IF (THI(I).GE.TKLO(IDENT,NTID)) GO TO 306
          JEND(I)=NTID
          NHI(I)=1.0
          FHI(I)=10000.
          GO TO 300
      306 CONTINUE
                DO 307 J=1,NTID
                IF (THI(I).GE.TKLO(IDENT,J).AND.THI(I).LT.TKHI(IDENT,J))
     -                    GO TO 308
      307       CONTINUE
                WRITE (6,962) I
      962       FORMAT (5X, 'FOR ', I2, 'TH LAYER, THI IS OUT OF BOUND')
      308       JEND(I)=J
                CALL FRAGMT(BT(IDENT,J),ET(IDENT,J),TKLO(IDENT,J),THI(I),
     -                HEATRT(IDENT,J),NKLO(IDENT,J),NHI(I))
                FHI(I)=1.0/(1.0-NHI(I))
      300 CONTINUE
C
C  REDEFINE AND RENUMBER THE SUBDIVIDED MULTILAYERS, BASED ON THE
C  TEMPERATURE RANGES OF THERMOCHEMICAL REGIMES AND ALSO ON THE GENERIC
C  DIVISIONS
C  SEQUENCE OF IJ IS FROM FRONT (HOTTEST) LAYER TO REAR (COLDEST) LAYER
C
          IJ=0
          DO 310 I=1,NLAYG
          IDENT=ID(I)
          JENDI=JEND(I)
          JSTAI=JSTART(I)
          IJ=IJ+1
          T(IJ)=THI(I)
          ANAME(IJ,1)=ANAMET(IDENT,1)
          ANAME(IJ,2)=ANAMET(IDENT,2)
          D(IJ)=DT(IDENT,JENDI)
          CP(IJ)=CPT(IDENT,JENDI)
          RHO(IJ)=RHOT(IDENT,JENDI)
          E(IJ)=ET(IDENT,JENDI)
          B(IJ)=BT(IDENT,JENDI)
          K(IJ)=KT(IDENT,JENDI)
          HEATRA(IJ)=HEATRT(IDENT,JENDI)
          NS(IJ)=NHI(I)
          FSS(IJ)=FHI(I)
          NC(IJ)=NKLO(IDENT,JENDI)
          FSC(IJ)=FKLO(IDENT,JENDI)
          IF (JENDI.EQ.JSTAI)  NC(IJ)=NLO(I)
          IF (JENDI.EQ.JSTAI)  FSC(IJ)=FLO(I)
          IF (JENDI.EQ.JSTAI)  GO TO 310
          JENDI1=JENDI+1
                DO 311 J=JENDI1,JSTAI
                IJ=IJ+1
                T(IJ)=TKHI(IDENT,J)
                ANAME(IJ,1)=ANAMET(IDENT,1)
                ANAME(IJ,2)=ANAMET(IDENT,2)
                D(IJ)=DT(IDENT,J)
                CP(IJ)=CPT(IDENT,J)
                RHO(IJ)=RHOT(IDENT,J)
                E(IJ)=ET(IDENT,J)
```

```
10*                   B(IJ)=BT(IDENT,J)
11*                   K(IJ)=KT(IDENT,J)
12*                   HEATRA(IJ)=HEATRT(IDENT,J)
13*                   NS(IJ)=NKHI(IDENT,J)
14*                   FSS(IJ)=FKHI(IDENT,J)
15*                   NC(IJ)=NKLO(IDENT,J)
16*                   FSC(IJ)=FKLO(IDENT,J)
17*                   IF (J.EQ.JSTAI)  NC(IJ)=NLO(I)
18*                   IF (J.EQ.JSTAI)  FSC(IJ)=FLO(I)
19*         311       CONTINUE
20*         310 CONTINUE
21*             NLAYER=IJ
22*             T(IJ+1)=TBACK
23*             WRITE (6,900) (I,ANAME(I,1),ANAME(I,2), T(I), K(I), CP(I), RHO(I),
24*            - B(I), E(I), D(I), HEATRA(I), I=1,NLAYER)
25*         900 FORMAT (5X, I2,2X, 2A5,  F6.1, 1X, F10.5,  4X, F6.3,  5X, F6.3,
26*            -    E14.3, 3X, F5.0, 4X,F7.0,F5.3 )
27*             WRITE (6,907) TBACK
28*         907 FORMAT (9X, 'REAR SURF', F6.0, // )
29*             WRITE (6, 910)
30*         910 FORMAT (5X, 'PREDICTED BURNING RATE' ///,20X, 'BURN RATE'
31*            -  '  SURFACE TEMP.  HEAT'
32*            - ' FLUX IN   HEAT FLUX OUT   HEAT CONSUMED    FS-TOP SURFACE'
33*            -    '    FS-BOTTOM' / 21X, '(CM/SEC)', 7X, '(K)', 7X,
34*            - 3( '(CAL/CM2SEC)', 3X ), //)
35*             NLAY1 = NLAYER - 1
36*             NCALC = 0
37*         C
38*         C     CALCULATE THE BURNING RATES FOR THE FIRST TIME ASSUMING THAT THE BURN
39*         C     RATE ARE THE SAME FOR EVERY LAYER
40*         C
41*             DO 333 I=1, NLAYER
42*                TIO(I) = T(I) - TO
43*             H(I) = D(I) / (CP(I) * (T(I)-TO))
44*             ALPHA(I) = K(I) / (RHO(I)*CP(I) )
45*             CHI(I) = (T(I)-TO) /T(I)
46*             THETA(I) = E(I)/(R*T(I))
47*             XIS(I) = -H(I) /FSS(I)
48*             XIC(I) = -H(I) /FSC(I)
49*             TAUC = (T(I+1) - TO) /(T(I) - TO)
50*             IF (T(I+1).LE.300.) GO TO 337
51*             ETAC(I) = THETA(I) * CHI(I) * (1.0 - TAUC)
52*             ENC(I) = EXP(-ETAC(I))
53*             HXICS=(H(I)+XIC(I)) / (H(I) + XIS(I) )
54*             LAMBDA(I) = (XIS(I)-XIC(I) + (1.0+H(I))*ALOG(HXICS))/(1.0-ENC(I))
55*             RSQ = K(I) * B(I) * EXP(-THETA(I)) / (RHO(I)*CP(I)* LAMBDA(I)*
56*            -    THETA(I) * CHI(I))
57*             IF (RSQ.LT.0.0) WRITE(6,950) I,RSQ,LAMBDA(I)
58*             IF (RSQ.LT.0.0) RSQ=-RSQ
59*             GO TO 500
60*         337 CONTINUE
61*             RSQ = ALPHA(I)*B(I)*EXP(-THETA(I))/(THETA(I)*CHI(I)*((1.0+H(I))*
62*            -  ALOG(FSS(I)/(FSS(I)-1.0)) + XIS(I)))
63*             IF (RSQ.LT.0.0) WRITE (6,950)I,RSQ,FSS(I)
64*             IF (RSQ.LT.0.0) RSQ=-RSQ
65*         500 CONTINUE
66*             RB(I) = SQRT(RSQ)
```

```
      PS(I) = -1.0 + XIS(I)
      QIN(I) =-PS(I) * TIO(I)    *RB(I)*RHO(I)*CP(I)
      PC(I) = -TAUC + XIC(I)
      QOUT(I) =-PC(I)* TIO(I)    * RB(I) *RHO(I) * CP(I)
      QNET(I) = QIN(I) - QOUT(I)
  333 CONTINUE
C
C     CALCULATE BURNING RATES SIMULTANEOUSLY FOR ALL THE LAYERS
C
  379 CONTINUE
      IF (KCALC.EQ.100) GO TO 777
      DO 381 I=1,NLAYER
         RBT(I) = RB(I)
         RORC(I) = RBT(I) * RHO(I) * CP(I)
      A(I) = RORC(I)*(T(I)-T(I+1)) + D(I)*RHO(I)*RBT(I)
     -  * (1./FSS(I) - 1./FSC(I) )
  381 CONTINUE
C     WRITE (6,924)
C 924 FORMAT (//4X,'I', 6X,'PS',11X,'XIS', 11X,'PC', 11),'XIC', 11X,'S',
C    -  11X,'ENC', 11X,'CK', 11X,'LAMBDA')
      DO 382 II=1,NLAY1
      I = NLAY1  + 1 - II
        PS(I) = 0.0
        DO 384 J=I, NLAYER
  384      PS(I) = PS(I) + A(J)
        PS(I) = -PS(I) / (TIO(I)*RORC(I))
      G(I) = - (PS(I) + 1.0 - H(I)*(1.0 - 1.0/FSS(I) ) )
         XIS(I) = PS(I) + 1.0
         PC(I) = PS(I) + A(I)/ (TIO(I)*RORC(I) )
         XIC(I) = PC(I) + (T(I+1)-TO)/TIO(I)
         ETAC(I) = (E(I)/R)*(T(I)-T(I+1))/(T(I)*T(I))
         ENC(I) = EXP(-ETAC(I))
      GXICS=(G(I)+XIC(I)) / (G(I) + XIS(I) )
      IF (GXICS.LT.0.0) WRITE (6,918) I,GXICS,G(I),XIC(I),XIS(I)
      IF (GXICS.LT.0.0) GO TO 777
  918 FORMAT (10X,'GXICS (',I2,')=',F15.6, 'XIC=',E15.6,'XIS=',E15.6)
      LAMBDA(I) = (XIS(I)-XIC(I) + (1.0+G(I))*ALOG(GXICS))/(1.0-ENC(I))
      RSQ = ALPHA(I)*P(I)*EXP(-THETA(I))/(LAMBDA(I)*THETA(I)*CPI(I))
      IF (RSQ.LT.0.0) RSQ=-RSQ
      RB(I) = SQRT(RSQ)
         RORC(I) = RB (I) * RHO(I) * CP(I)
         A(I) = RORC(I)*(T(I)-T(I+1)) + D(I)*RHO(I)*RB (I)
     -           * (1./FSS(I) - 1./FSC(I) )
C     WRITE (6,925) I,PS(I),XIS(I),PC(I),XIC(I),G(I),ENC(I),
C    - LAMBDA(I)
C 925 FORMAT (3X, I2, 8(3X,E10.5) )
C     QIN(I) =- PS(I) * (T(I)-TO)*RB(I)*RHO(I)*CP(I)
C     QOUT(I) = -PC(I)*(T(I)-TO) * RB(I) *RHO(I) * CP(I)
C     QNET(I) = QIN(I) - QOUT(I)
  382 CONTINUE
C     WRITE (6,920) (I, ANAME(I,1), ANAME(I,2), RB(I), T(I),
C    -   QIN(I), QOUT(I), QNET(I), FSS(I), FSC(I),I=1,NLAYER)
C
C  STOP IF CONVERGED ENOUGH OR KEEP ITERATIVE CALCULATION
C
      DO 386 I=1,NLAYER
      IF (ABS(RBT(I)/RB(I)-1.0).LT.0.01)  GO TO 386
```

```
24*           NCALC = NCALC + 1
25*           GO TO 379
26*       386 CONTINUE
27*       777 CONTINUE
28*           WRITE (6,928) NCALC
29*       928 FORMAT (2X, 'NO OF ITERATION = ', I3, /)
30*           DO 388 I=1,NLAYER
31*           QIN(I) =- PS(I) * (T(I)-TO)*RB(I)*RHO(I)*CP(I)
32*           QOUT(I) = -PC(I)*(T(I)-TO) * RB(I) *RHO(I) * CP(I)
33*           QNET(I) = QIN(I) - QOUT(I)
34*       388 CONTINUE
35*           WRITE (6,920) (I, ANAME(I,1), ANAME(I,2), RB(I), T(I),
36*          -   QIN(I), QOUT(I), QNET(I), FSS(I), FSC(I),I=1,NLAYER)
37*       920 FORMAT (5X,I2,2X,2A5,F10.5, 2X, F10.1, 3X, F10.4, 6X, F10.4, 6X,
38*          -    F10.4, 8X, E10.5, 8X, E10.5 /)
39*       950 FORMAT (10X,'RSQ (',I2, ')= ', E13.5, 10X, E13.5)
40*           WLOSS=0.0
41*           DO 393 I=1,NLAYER
42*       393 WLOSS=WLOSS+RB(I)*RHO(I)*(1./FSS(I)-1./FSC(I))
43*           WRITE (6,927) WLOSS
44*       927 FORMAT (///, '   WEIGHT LOSS PREDICTED BY THE MODEL', /,3',34('=')
45*          -, /, 40X,F10.5, ' GRAM/SEC.CM2 OF BURNING SURFACE ' )
46*     C
47*     C  PRELIMINARY CALCULATION BEFORE PLOTTING T VS X
48*     C
49*           DO 1120 I=1,NLAYER
50*           TINTV(I)=(T(I)-T(I+1))/FLOAT(10)
51*           TP(I,1)=T(I)
52*           DO 1121 J=1,10
53*           TP(I,J+1)=T(I)-TINTV(I)*FLOAT(J)
54*      1121 CONTINUE
55*      1120 CONTINUE
56*           DO 1210 I=1,NLAYER
57*           NSSP(I,11)=NC(I)
58*           DO 1220 JJ=2,11
59*           J=12-JJ
60*           IF(TP(I,J).LE.TSTART(I)) NSSP(I,J)=1.0
61*           IF(TP(I,J).LE.TSTART(I)) GO TO 1220
62*           CALL FRAGMT(B(I),E(I),TP(I,11),TP(I,J),HEATRA(I),NSSP(I,11),
63*          - NSSP(I,J))
64*      1220 CONTINUE
65*      1210 CONTINUE
66*           RHS(NLAYER,11)=0.00001
67*           DO 1310 II=1,NLAYER
68*           I=NLAYER+1-II
69*           RHORB =RHO(I)*RB(I)
70*           DO 1320 JJ=2,11
71*           J=12-JJ
72*           DTDXK=RHORB*(CP(I)*(TP(I,J)-TP(I,J+1))
73*          -                                    + D(I)*(NSSP(I,J+1)-NSSP(I,J)))
74*           RHS(I,J)=DTDXK+RHS(I,J+1)
75*           DXDT(I,J)=K(I)/RHS(I,J)
76*      1320 CONTINUE
77*           RHS(I-1,11)=RHS(I,J)
78*      1310 CONTINUE
79*           SUM=0.0
80*           DO 1330 II=1,NLAYER
```

```
81*            I=NLAYER+1-II
82*            DO 1330 JJ=1,9,2
83*            J=12-JJ
84*            DX(I,J-2)=(DXDT(I,J)+4.*DXDT(I,J-1)+DXDT(I,J-2))*TINTV(I)/3.
85*            SUM=SUM+DX(I,J-2)
86*            X(I,J-2)=SUM
87*         1330 CONTINUE
88*        C  CLEAR THE MEMORIES OF XPLOT AND TPLOT
89*            DO 1338 I=1,121
90*            XPLOT(I)=0.0
91*         1338 TPLOT(I)=0.0
92*            DO 1340 I=1,NLAYER
93*            DO 1340 JJ=1,5
94*            IND=(I-1)*5 + JJ
95*            J=JJ*2-1
96*            XPLOT(IND)=SUM - X(I,J)
97*            TPLOT(IND)=TP(I,J)
98*         1340 CONTINUE
99*            IND=IND+1
00*            XPLOT(IND)=SUM
01*            TPLOT(IND)=TP(I,J+2)
02*            IPLOT=IPLOT+1
03*            IF (IPLOT.GT.5) IPLOT=1
04*            IF (IPLOT.EQ.1.AND.NPLOT.NE.NPAGE) CALL ADVPLT
05*            CALL PLFORM ('LINLIN',2.5,2.75)
06*            CALL PLABEL ('TEMPERATURE PROFILE',  0,
07*           -  'DEPTH FROM SURFACE (CM)',  0, 'TEMPERATURE (K)',  0)
08*            CALL PLSCAL ((0.0,10.0),2,100000,(300.0,800.0),2,100000)
09*            CALL PLCSIZ(0.06,0.0)
10*            GO TO (1341,1342,1343,1344,1345), IPLOT
11*         1341 CALL ORIGIN (1.0,4.3)
12*            GO TO 1348
13*         1342 CALL ORIGIN (3.0,0.0)
14*            GO TO 1348
15*         1343 CALL ORIGIN (3.0,0.0)
16*            GO TO 1348
17*         1344 CALL ORIGIN (-6.0,-3.1)
18*            GO TO 1348
19*         1345 CALL ORIGIN (3.0,0.0)
20*            NPLOT=NPLOT+1
21*         1348 CALL PLGRAF
22*            CALL PLCURV (XPLOT,TPLOT,121,0,'+')
23*            GO TO 1111
24*         1112 CONTINUE
25*            CALL ENDPLT
26*            STOP
27*            END
```

```
1*              SUBROUTINE FRAGMT(SB,SE,STI,STF,SHR,SNI,SNF)
2*              DOUBLE PRECISION SX1,SX2,SY1,SY2,DEI
3*              STHI=SE/(1.98717*STI)
4*              STHF=SE/(1.98717*STF)
5*              SA1=EXP(-STHF)*STF - EXP(-STHI)*STI
6*              SX1 = -STHI
7*              SX2 = -STHF
8*              SY1=DEI(SX1)
9*              SY2=DEI(SX2)
10*             SA2= SY2-SY1
11*             SNF=SNI*EXP(-(SA1+SE/1.98717*SA2)*SB/SHR)
12*             RETURN
13*             END
```

BURNING RATE PREDICTION FOR MULTI-LAYERED AIRCRAFT SEAT CUSHION

MATERIAL PROPERTY	TEMP. RANGE. (K)	THERMAL CONDUCTIV. (CAL/CM.S.C)	HEAT CAPACITY (CAL/GM.C)	DENSITY (GM/CM3)	PREEXP. FACTOR	ACTIVATION ENERGY (CAL/MOLE)	HEAT OF DECOMPOS. (CAL/GM)	HEAT RATE (DEG C/SEC)
1 COVER FABR								
	848.2- 898.2	.00010	.600	.400	.213+05	24800.	-2.9	.33
	813.2- 848.2	.00010	.600	.400	.506-07	-20300.	-2.9	.33
	763.2- 813.2	.00010	.600	.400	.224+14	56500.	-2.9	.33
	689.2- 763.2	.00010	.600	.400	.251+00	7800.	-2.9	.33
	602.2- 689.2	.00010	.600	.400	.730-05	-6500.	-16.3	.33
	523.2- 602.2	.00010	.600	.400	.157+03	13700.	-16.3	.33
2 VONAR								
	881.0- 923.0	.00020	.345	.146	.337-03	1043.	1.0	.33
	766.0- 881.0	.00020	.345	.146	.166-06	-12285.	9.6	.33
	709.0- 766.0	.00020	.345	.146	.894-01	7800.	-23.9	.33
	661.0- 709.0	.00020	.345	.146	.237-11	-26532.	-28.7	.33
	623.0- 661.0	.00020	.345	.146	.275+05	22078.	-28.7	.33
	591.0- 623.0	.00020	.345	.146	.394-12	-25933.	50.9	.33
	473.0- 591.0	.00020	.345	.146	.233+05	19435.	107.5	.33
3 LS 200								
	876.6- 923.0	.00020	.300	.120	.117-04	-3857.	.5	.33
	766.6- 876.6	.00020	.300	.120	.717-10	-24770.	9.6	.33
	723.0- 766.6	.00020	.300	.120	.517+02	16818.	-8.4	.33
	698.0- 723.0	.00020	.300	.120	.104-03	-2020.	-19.1	.33
	673.0- 698.0	.00020	.300	.120	.828-13	-31083.	-16.7	.33
	648.0- 673.0	.00020	.300	.120	.656-02	2475.	-8.4	.33
	623.0- 648.0	.00020	.300	.120	.246+07	27897.	-20.3	.33
	598.0- 623.0	.00020	.300	.120	.161-16	-38190.	7.9	.33
	573.0- 598.0	.00020	.300	.120	.211+08	27800.	71.7	.33
	548.0- 573.0	.00020	.300	.120	.201+00	6772.	24.9	.33
	473.0- 548.0	.00020	.300	.120	.783+04	18279.	54.9	.33
4 PREOX								
	873.0- 908.0	.00010	.300	.620	.542-05	-13061.	.5	.33
	848.0- 873.0	.00010	.300	.620	.855+21	91578.	.5	.33
	748.0- 848.0	.00010	.300	.620	.155+03	18860.	.5	.33
	683.0- 748.0	.00010	.300	.620	.985-02	4500.	-13.9	.33
	623.0- 683.0	.00010	.300	.620	.143-04	-4365.	-13.9	.33
	573.0- 623.0	.00010	.300	.620	.587-02	3085.	-13.9	.33
	498.0- 573.0	.00010	.300	.620	.594+01	10963.	.5	.33
5 PU FOAM								
	644.0- 688.0	.00010	.400	.030	.844+20	65757.	3.1	.33
	598.0- 644.0	.00010	.400	.030	.617+02	12335.	11.9	.33
	573.0- 598.0	.00010	.400	.030	.177-01	2646.	2.5	.33
	544.0- 573.0	.00010	.400	.030	.260+06	21435.	2.5	.33
	448.0- 544.0	.00010	.400	.030	.600+01	9900.	.5	.33
6 IMIDE FOAM								
	1006.0- 1073.0	.00010	.200	.023	.306-04	-4763.	.5	.33
	973.0- 1006.0	.00010	.200	.023	.312-13	-46170.	.5	.33
	915.0- 973.0	.00010	.200	.023	.180-06	-16074.	.5	.33
	854.0- 915.0	.00010	.200	.023	.133+02	16862.	-7.3	.33
	796.0- 854.0	.00010	.200	.023	.611-05	-7889.	-7.3	.33
	711.0- 796.0	.00010	.200	.023	.107+08	36705.	-7.0	.33
	673.0- 711.0	.00010	.200	.023	.763-02	6938.	-.3	.33

NORMALIZED FRAGMENT SIZE AT END TEMPS OF KINETIC REGIMES

1	COVER FABR				
		523.2- 602.2	1.000000	--	.821322
		602.2- 689.2	.821322	--	.602183
		689.2- 763.2	.602183	--	.467861
		763.2- 813.2	.467861	--	.193770
		813.2- 848.2	.193770	--	.059566
		848.2- 898.2	.059566	--	.007807
2	VONAR				
		473.0- 591.0	1.000000	--	.865850
		591.0- 623.0	.865850	--	.793600
		623.0- 661.0	.793600	--	.718568
		661.0- 709.0	.718568	--	.644733
		709.0- 766.0	.644733	--	.598173
		766.0- 881.0	.598173	--	.535456
		881.0- 923.0	.535456	--	.522900
3	LS 200				
		473.0- 548.0	1.000000	--	.967082
		548.0- 573.0	.967082	--	.934163
		573.0- 598.0	.934163	--	.871674
		598.0- 623.0	.871674	--	.820223
		623.0- 648.0	.820223	--	.781499
		648.0- 673.0	.781499	--	.725286
		673.0- 698.0	.725286	--	.688495
		698.0- 723.0	.688495	--	.666312
		723.0- 766.6	.666312	--	.615242
		766.6- 876.6	.615242	--	.550394
		876.6- 923.0	.550394	--	.542658
4	PREOX				
		498.0- 573.0	1.000000	--	.953137
		573.0- 623.0	.953137	--	.892503
		623.0- 683.0	.892503	--	.829126
		683.0- 748.0	.829126	--	.763548
		748.0- 848.0	.763548	--	.542460
		848.0- 873.0	.542460	--	.367852
		873.0- 908.0	.367852	--	.146867
5	PU FOAM				
		448.0- 544.0	1.000000	--	.918863
		544.0- 573.0	.918883	--	.834678
		573.0- 598.0	.834678	--	.727952
		598.0- 644.0	.727952	--	.490399
		644.0- 688.0	.490399	--	.006318
6	IMIDE FOAM				
		673.0- 711.0	1.000000	--	.994404
		711.0- 796.0	.994404	--	.917053
		796.0- 854.0	.917053	--	.803906
		854.0- 915.0	.803906	--	.679453
		915.0- 973.0	.679453	--	.574808
		973.0- 1006.0	.574808	--	.546754
		1006.0- 1073.0	.546754	--	.513983

BURNING RATE PREDICTION FOR MULTI-LAYERED AIRCRAFT SEAT CUSHION

RUN NO. 19 0.5 INCH LS-200 T=6 MIN

	MATERIAL	SURFACE TEMP. (K)	THERMAL CONDUCTIV. (CAL/CM.S.C)	HEAT CAPACITY (CAL/GM.C)	DENSITY (GM/CM3)	PREEXP. FACTOR	ACTIVATION ENERGY (CAL/MOLE)	HEAT OF DECOMPOS. (CAL/GM)	HEAT RATE (DEG C/SEC)
1	COVER FABR	691.0	.00010	.600	.400	.251+00	7800.	-3.	.333
2	COVER FABR	659.2	.00010	.600	.400	.730-05	-6500.	-16.	.333
3	LS 200	677.0	.00020	.300	.120	.828-13	-31083.	-17.	.333
4	LS 200	673.0	.00020	.300	.120	.656-02	2475.	-8.	.333
5	LS 200	648.0	.00020	.300	.120	.246+07	27897.	-20.	.333
6	LS 200	623.0	.00020	.300	.120	.161-16	-38190.	8.	.333
7	LS 200	598.0	.00020	.300	.120	.211+08	27800.	72.	.333
8	LS 200	573.0	.00020	.300	.120	.201+00	6772.	25.	.333
9	LS 200	548.0	.00020	.300	.120	.783+04	18279.	55.	.333
10	PU FOAM	459.0	.00010	.400	.030	.600+01	9900.	1.	.333
	REAR SURF	291.							

PREDICTED BURNING RATE

		BURN RATE (CM/SEC)	SURFACE TEMP. (K)	HEAT FLUX IN (CAL/CM2SEC)	HEAT FLUX OUT (CAL/CM2SEC)	HEAT CONSUMED (CAL/CM2SEC)	FS-TOP SURFACE	FS-BOTTOM
NO OF ITERATION =	5							
1	COVER FABR	.00083	691.0	.0400	.0396	.0004	.24964+01	.25137+01
2	COVER FABR	.00084	689.2	.0396	.0372	.0024	.25137+01	.26443+01
3	LS 200	.00180	677.0	.0369	.0367	.0002	.35333+01	.36401+01
4	LS 200	.00181	673.0	.0367	.0352	.0015	.36401+01	.45766+01
5	LS 200	.00191	648.0	.0352	.0337	.0015	.45766+01	.55624+01
6	LS 200	.00194	623.0	.0337	.0318	.0018	.55624+01	.77926+01
7	LS 200	.00215	598.0	.0319	.0288	.0031	.77926+01	.15189+02
8	LS 200	.00234	573.0	.0288	.0264	.0023	.15189+02	.30379+02
9	LS 200	.00281	548.0	.0265	.0168	.0096	.30379+02	.10000+05
10	PU FOAM	.00836	459.0	.0174	.0006	.0168	.29784+03	.10000+05

WEIGHT LOSS PREDICTED BY THE MODEL .00008 GRAM/SEC.CM2 OF BURNING SURFACE

```
C                                  PROGRAM B
C  THIS PROGRAM TAKES THE TEMPERATURE AND CONDUCTIVE HEAT FLUX AT THE
C  FRONT (HOT) SURFACE (I.E., B.C.'S) AS THE INPUT DATA AND THEN CALCULATES
C  THE BURNING RATE, TEMPERATURE PROFILE, AND WEIGHT LOSS OF MULTI-LAYERED
C  POLYMERIC MATERIALS (INCLUDING FIRE BLOCKING LAYER) USED FOR AIRCRAFT
C  SEAT CUSHIONS.
C  THE DIMENSIONS USED IN THIS PROGRAM ARE GRAM, GRAM-MOLE, D-CELSIUS,
C  CALORIE, CM, AND SECOND.
C
      COMMON /TCM1/ANAMET(7,2),MW( 7),NTREG( 7),KT(7,11),CPT(7,11),
     1  RHOT(7,11),BT(7,11),ET(7,11),DT(7,11),HEATRT(7,11),TKLO(7,11),
     2  TKHI(7,11),TS(201),N(201),FS(201),QS(201),RR(201),X(201),
     3  NKLO(7,11),NKHI(7,11),FKLO(7,11),FKHI(7,11),ID(8),THICK(8),
     4  RHO(201),LAMBDA,R,I,IDI,TC,J1
      REAL KT, N, NKHI, NKLO, LAMBDA,MW
      DIMENSION HEADIN(16),WLOSS(7)
C
C  READ IN THE INGREDIENT MATERIAL PROPERTY AND PRINT OUT
C
      READ (5,901) ITOTAL
  901 FORMAT (I2)
      DO 100  II=1,ITOTAL
            READ (5,902) I,ANAMET(I,1),ANAMET(I,2),MW(I),NTREG(I)
  902       FORMAT(I2,2A5,F10.2,I2)
            NTR=NTREG(I)
            READ (5,903)(TKLO(I,J),TKHI(I,J),KT(I,J),CPT(I,J),RHOT(I,J),
     -                  BT(I,J),ET(I,J),DT(I,J),HEATRT(I,J),J=1,NTR)
  903       FORMAT (2F5.1, 7E10.3)
  100 CONTINUE
      WRITE (6,948)
  948 FORMAT (1H1, 25X, 'BURNING RATE PREDICTION FOR MULTI-LAYERED'
     - ' AIRCRAFT SEAT CUSHION' / 26X, 63('='), /
     -      5X, 'MATERIAL PROPERTY'/  21X, 'TEMP. RANGE.   THERMAL', 5X,
     - 'HEAT', 6X,'DENSITY    PREEXP.    ACTIVATION   HEAT OF    HEAT',
     - 5X      / 36X, 'CONDUCTIV.  CAPACITY',13X, 'FACTOR     ENERGY',
     - 7X, 'DECOMPOS.  RATE', /
     -26X, '(K)', 5X,'(CAL/CM.S.C)  (CAL/GM.C) (GM/CM3)', 13X,
     -'(CAL/MOLE)   (CAL/GM)   (DEG C/SEC)'  /)
      DO 102 I=1,ITOTAL
      NTR=NTREG(I)
      WRITE (6,951)  I,ANAMET(I,1),ANAMET(I,2)
  951 FORMAT (5X,I2,2X,2A5)
      WRITE (6,953) (TKLO(I,J),TKHI(I,J),
     -  KT(I,J),CPT(I,J),RHOT(I,J),BT(I,J),ET(I,J),DT(I,J),HEATRT(I,J),
     -      J=1,NTR)
  953 FORMAT (17X, F7.1, '-', F7.1, 1X,
     -      F10.5,3X, F6.3, 3X, F6.3, 2X, E11.3, 4X, F9.0, F10.1, F10.2)
  102 CONTINUE
C
C  FIX CONSTANTS USED IN THIS PROGRAM
```

```
51*      C
52*            P=1.0
53*            R=1.98717
54*            RM=82.06
55*            CPGAS=0.382
56*            EPSLON=0.9
57*            SIGMA=1.355E-12
58*            TO=285.0
59*      C
60*      C  CALCULATE N AND FS  AT TWO END TEMPERATURES OF KINETIC REGIMES
61*      C  THE CALCULATION SEQUENCE IS, BY LOGIC, FROM LOW TO HIGH TEMPERATURE
62*      C
63*            WRITE (6,955)
64*        955 FORMAT (1H1, 10X, 'NORMALIZED FRAGMENT SIZE AT END TEMPS OF', 1X,
65*           - 'KINETIC REGIMES', /, 11X, 56('='), /)
66*            DO 200 I=1,ITOTAL
67*                  WRITE (6,951) I, ANAMET(I, 1), ANAMET(I,2)
68*                  NTR=NTREG(I)
69*                  NKLO(I,NTR)=1.0
70*                  FKLO(I,NTR)=10000.
71*            DO 205 JJ=1,NTR
72*               J=NTR+1-JJ
73*                  CALL FRAGMT (BT(I,J),ET(I,J),TKLO(I,J),TKHI(I,J),
74*           -            HEATRT(I,J),NKLO(I,J),NKHI(I,J))
75*                  IF (J.NE.1) NKLO(I,J-1)=NKHI(I,J)
76*                  IF (NKLO(I,J).EQ.1.0) NKLO(I,J)=0.9999999
77*                  FKLO(I,J) = 1.0/(1.0-NKLO(I,J))
78*                  IF (NKHI(I,J).EQ.1.0) NKHI(I,J)=0.9999999
79*                  FKHI(I,J) = 1.0/(1.0-NKHI(I,J))
80*                  WRITE (6,958) TKLO(I,J),TKHI(I,J),NKLO(I,J),NKHI(I,J)
81*        958 FORMAT (22X, F7.1, '-', F7.1, 5X, F11.6, 2X, '--', 1X, F11.6)
82*        205 CONTINUE
83*        200 CONTINUE
84*      C
85*      C  INITIALLIZE A FEW VARIABLES FOR COMPUTER PLOTTING
86*      C
87*            NPAGE=9
88*            NPLOT=1
89*            IPLOT=0
90*            CALL BGNPLT
91*      C
92*      C  READ IN THE INPUT DATA, I.E., TOTAL NUMBER OF LAYERS AND THEIR ORDER
93*      C  THICKNESS OF EACH LAYER (CM), AND FRONT SURFACE HEAT FLUX
94*      C  AND FRONT SURFACE TEMPERATURE (K)
95*      C
96*       1112 CONTINUE
97*      C  CLEAR THE MEMORIES OF PLOT
98*            DO 1338 I=1,201
99*            X(I)=0.0
00*       1338 TS(I)=0.0
01*            READ (5,907,END=1110) (HEADIN(I),I=1,16)
02*        907 FORMAT (16A5)
03*            READ (5,904)  NLAYG,(ID(I),I=1,NLAYG)
04*            READ (5,905) (THICK(I),I=1,NLAYG)
05*            READ (5,906) QS1,TS1
06*        904 FORMAT (16I5)
07*        905 FORMAT (8F10.0)
```

```
      906 FORMAT(2F10.0)
          WRITE (6,959) (HEADIN(I),I=1,16)
      959 FORMAT (1H1,20X,16A5/)
          WRITE (6,960)
      960 FORMAT (10X, *MATERIAL / THICKNESS*,/)
          DO 250 I=1,NLAYG
          IDI=ID(I)
      250 WRITE (6,961) ANAMET(IDI,1), ANAMET(IDI,2), THICK(I)
      961 FORMAT (20X, 2A5, 5X, F5.1, * CM*,/)
          WRITE (6,964) QS1,TS1
      964 FORMAT (10X, *BOUNDARY CONDITION*,/, 20X, *HEAT FLUX (CONDUCTIVE)*
         - ,* =*, F10.4, * CAL/CM2.SEC*, /, 20X, *SURFACE TEMPERATURE    =*,
         -  F6.1, * K*, /)
C
C  THE DIMENSIONS FOR TS, X, QS, N, RB HAVE TO BE LARGE ENOUGH TO COVER THE
C  WHOLE TEMPERATURE DROP FROM THE FRONT TO REAR SURFACE IS COVERED
C  WITH THE TEMPERATURE INTERVAL (TINTV) AS SHOWN BELOW
C
          TINTV=4.0
          I=0
          TS(1)=TS1
          QS(1)=QS1
          X(1)=0.0
          STHICK=0.0
          TWLT=0.0
          DO 251 ING=1,7
      251 WLOSS(ING)=0.0
          WRITE (6,965)
      965 FORMAT (11X,*I*, 9X, *RB*, 5X, *TS(I) - TS(I+1)*,  8X, *DX*,
         -  5X, *X(I) - X(I+1)*, 5X,*QS(I)   QS(I+1)*, 10X,*N(I)   N(I+1)*/)
          DO 500 III=1,NLAYG
          I1=I+1
          IDI=ID(III)
          WRITE (6,970) III, ANAMET(IDI,1), ANAMET(IDI,2)
      970 FORMAT (3X, I3, 3X,2A5)
          NTR=NTREG(IDI)
          STHICK=STHICK+THICK(III)
      502 CONTINUE
          I=I+1
          TS(I+1)=TS(I) - TINTV
      504 CONTINUE
          IF (TS(I+1).LT.TO) TS(I+1)=TO
          IF(TS(I).LE.TKLO(IDI,NTR)) N(I)=1.0
          IF(TS(I).LE.TKLO(IDI,NTR)) GO TO 310
          DO 307 J=1,NTR
          IF (TS(I).GT.TKLO(IDI,J).AND.TS(I).LE.TKHI(IDI,J)) GO TO 308
      307 CONTINUE
      308 J1=J
          IF (TS(I+1).LT.TKLO(IDI,J1))  TS(I+1)=TKLO(IDI,J1)
          CALL FRAGMT (BT(IDI,J),ET(IDI,J),TKLO(IDI,J),TS(I),
         1            HEATRT(IDI,J),NKLO(IDI,J),N(I))
          IF (N(I).EQ.1.0) FS(I)=10000.
          IF (N(I).NE.1.0)  FS(I)=1.0/(1.0-N(I))
          CALL FRAGMT (BT(IDI,J),ET(IDI,J),TKLO(IDI,J),TS(I+1),
         1             HEATRT(IDI,J),NKLO(IDI,J),N(I+1))
          IF (N(I+1).EQ.1.0) FS(I+1)=10000.
          IF (N(I+1).NE.1.0) FS(I+1)=1.0/(1.0-N(I+1))
```

```
65*      C
66*      C  CALCULATE THE BURNING RATE R USING THE HEAT FLUX AT THE FRONT
67*      C  AND THE ASSUMED HEAT FLUX (VIA REAR SURFACE TEMPERATURE)
68*      C
69*            CALL BURNRT
70*            RHO(I)=RHOT(IDI,J1)
71*            DTDX=QS(I)/KT(IDI,J1)
72*            DX=(TS(I)-TS(I+1))/DTDX
73*            GO TO 405
74*          310 CONTINUE
75*            IF (TS(I+1).LE.TKLO(IDI,NTR)) N(I+1)=1.0
76*            DENOM=RHOT(IDI,NTR)*CPT(IDI,NTR)*(TS(I)-T0)
77*            RB(I)=QS(I)/DENOM
78*            DX=KT(IDI,NTR)*(TS(I)-TS(I+1))/(DENOM*RB(I))
79*            RHO(I)=RHOT(IDI,NTR)
80*            QS(I+1)=QS(I)-RHOT(IDI,NTR)*RB(I)*CPT(IDI,NTR)*(TS(I)-TS(I+1))
81*          405 CONTINUE
82*            X(I+1)=X(I)+DX
83*            IF (ABS(X(I+1)/STHICK-1.0).LT.0.01) GO TO 499
84*            IF (ABS(QS(I+1)).LE.1.0E-04) GO TO 499
85*            IF (ABS(TS(I+1)/T0-1.0).LT.0.0035) GO TO 499
86*            IF (X(I+1).LT.STHICK.AND.QS(I+1).GT.0.0) WRITE (6,972) I,RB(I),
87*           -     TS(I),TS(I+1),DX,X(I),X(I+1),QS(I),QS(I+1),N(I),N(I+1)
88*          972 FORMAT(10X, I3, F10.5,  3X, F6.1, ' --', F6.1, 5X, F6.2, F8.4,'-',
89*           -       F8.4, 2X, F10.4, F10.4, 2X, F10.5,F10.5)
90*            IF (X(I+1).LT.STHICK.AND.QS(I+1).GT.0.0) GO TO 502
91*            IF (X(I+1).GE.STHICK) PFACT=(STHICK-X(I))/DX
92*            IF (QS(I+1).LE.0.0)  PFACT=QS(I)/(QS(I)-QS(I+1))
93*            TS(I+1)=TS(I)-(TS(I)-TS(I+1))*PFACT
94*            GO TO 504
95*          499 CONTINUE
96*            WRITE (6,972) I,RB(I),TS(I),TS(I+1),
97*           1     DX,X(I),X(I+1),QS(I),QS(I+1),N(I),N(I+1)
98*      C  ***NOTE*** N(I+1) OF ABOVE WILL BE REPLACED BY THE FIRST OF THE NEXT LAY
99*            I2=I
00*            DO 600 J=I1,I2
01*            WLT=RB(J)*RHO(J)*(N(J+1)-N(J))
02*            IF (WLT.LT.0.0) WRITE(6,976) J,WLT,WLOSS(III)
03*          976 FORMAT (10X, 'WLT(', I2, ')=',F10.5, '   WLOSS=',F10.5)
04*          600 WLOSS(III)=WLOSS(III)+WLT
05*            TWLT=TWLT+WLOSS(III)
06*          500 CONTINUE
07*            WRITE (6,982) (III,WLOSS(III),III=1,NLAYG)
08*          982 FORMAT (10X, 'MASS LOSS FOR ',  I3, ' LAYER=', E11.4,/
09*           -(24X,  I3, ' LAYER=',E11.4/))
10*            WRITE (6,977) TWLT
11*          977 FORMAT (2X,5('**'), '  TOTAL MASS LOSS =',E11.4, ' GM/SEC.CM2 OF '
12*           -  'BURNING SURFACE')
13*            IPLOT=IPLOT+1
14*            IF (IPLOT.GT.5) IPLOT=1
15*            IF (IPLOT.EQ.1.AND.NPLOT.NE.NPAGE) CALL ADVPLT
16*            CALL PLFORM ('LINLIN',2.5,2.75)
17*            CALL PLABEL ('TEMPERATURE PROFILE',  0,
18*           -  'DEPTH FROM SURFACE (CM)',  0, 'TEMPERATURE (K)',  0)
19*            CALL PLSCAL ((0.0,10.0),2,100000,(300.0,800.0),2,100000)
20*            CALL PLCSIZ(0.06,0.0)
21*            GO TO (1341,1342,1343,1344,1345), IPLOT
```

```
      1341 CALL ORIGIN (1.0,4.3)
           GO TO 1348
      1342 CALL ORIGIN (3.0,0.0)
           GO TO 1348
      1343 CALL ORIGIN (3.0,0.0)
           GO TO 1348
      1344 CALL ORIGIN (-6.0,-3.1)
           GO TO 1348
      1345 CALL ORIGIN (3.0,0.0)
           NPLOT=NPLOT+1
      1348 CALL PLGRAF
           CALL PLCURV (X,TS,201,0,'+')
           GO TO 1112
      1110 CONTINUE
           CALL ENDPLT
           STOP
           END
```

```
           SUBROUTINE FRACRT(SB,SE,STI,STF,SHR,SNI,SNF)
           DOUBLE PRECISION SX1,SX2,SY1,SY2,DEI
           STHI=SE/(1.98717*STI)
           STHF=SE/(1.98717*STF)
           SA1=EXP(-STHF)*STF - EXP(-STHI)*STI
           SX1 = -STHI
           SX2 = -STHF
           SY1=DEI(SX1)
           SY2=DEI(SX2)
           SA2= SY2-SY1
           SNF=SNI*EXP(-(SA1+SE/1.98717*SA2)*SB/SHR)
           RETURN
           END
```

```
           SUBROUTINE BURART
           COMMON /TCM1/ANAMET(7,2),MW( 7),NTREG( 7),KT(7,11),CPT(7,11),
          1  RHOT(7,11),DT(7,11),ET(7,11),DT(7,11),HEATRT(7,11),TKLO(7,11),
          2  TKHI(7,11),TS(201),N(201),FS(201),QS(201),RR(201),X(201),
          3  NKLO(7,11),NKHI(7,11),FKLO(7,11),FKHI(7,11),ID(9),THICK(8),
          4  RHO(201),LAMBDA,R,I,IDI,T0,J1
           REAL KT, N, NKHI, NKLO, LAMBDA,MW
           IF (I.EQ.1) RR(I)=0.001
           IF (I.NE.1) RR(I)=RR(I-1)
           IF (N(I).EQ.1.0) GO TO 378
       377 CONTINUE
           RRT=RR(I)
           PS=-QS(I)/((TS(I)-T0)*RR(I)*RHOT(IDI,J1)*CPT(IDI,J1))
           H=DT(IDI,J1)/(CPT(IDI,J1)*(TS(I)-T0))
           G=-PS-1.0+H*N(I)
           THETA=ET(IDI,J1)/(R*TS(I))
           ETAC=(ET(IDI,J1)/R)*(TS(I)-TS(I+1))/(TS(I)*TS(I))
```

```
18*            ENC=EXP(-ETAC)
19*            CHI=(TS(I)-TC)/TS(I)
20*            ALPHA=KT(IDI,J1)/(RHOT(IDI,J1)*CPT(IDI,J1))
21*            LAMBDA=(H*(N(I)-N(I+1))+(1.0+G)*ALOG(N(I+1)/N(I)))/(1.0-ENC)
22*            RSQ=ALPHA*BT(IDI,J1)*EXP(-THETA)/(LAMBDA*THETA*CHI)
23*            IF (RSQ.LT.0.0) WRITE (6,918) I,TS(I),TS(I+1),RSQ
24*          918 FORMAT (3X,'I=',I3,' TS(I)=',F6.1,' TS(I+1)=', F6.1,' RSQ=',
25*             1  E10.4/)
26*            IF (RSQ.LT.0.0) RSQ=-RSQ
27*            RB(I)=SQRT(RSQ)
28*            IF (ABS(RBT/RB(I)-1.0).GT.0.005) GO TO 377
29*          378 CONTINUE
30*            GS(I+1)=GS(I)-RB(I)*RHOT(IDI,J1)*(CPT(IDI,J1)*(TS(I)-TS(I+1))
31*             1       +DT(IDI,J1)*(N(I+1)-N(I)))
32*            RETURN
33*            END
```

BURNING RATE PREDICTION FOR MULTI-LAYERED AIRCRAFT SEAT CUSHION

MATERIAL PROPERTY	TEMP. RANGE. (K)	THERMAL CONDUCTIV. (CAL/CM.S.C)	HEAT CAPACITY (CAL/GM.C)	DENSITY (GM/CM3)	PREEXP. FACTOR	ACTIVATION ENERGY (CAL/MOLE)	HEAT OF DECOMPOS. (CAL/GM)	HEAT RATE (DEG C/SEC)
1 COVER FABR								
	848.2- 898.2	.00010	.300	.400	.213+05	24800.	-2.9	.33
	813.2- 848.2	.00010	.300	.400	.506-07	-20300.	-2.9	.33
	763.2- 813.2	.00010	.300	.400	.224+14	56500.	-2.9	.33
	689.2- 763.2	.00010	.300	.400	.251+00	7800.	-2.9	.33
	602.2- 689.2	.00010	.300	.400	.730-05	-6500.	-16.3	.33
	523.2- 602.2	.00010	.300	.400	.157+03	13700.	-16.3	.33
2 VONAR								
	881.0- 923.0	.00020	.345	.146	.337-03	1043.	1.0	.33
	766.0- 881.0	.00020	.345	.146	.166-06	-12285.	9.6	.33
	709.0- 766.0	.00020	.345	.146	.894-01	7800.	-23.9	.33
	661.0- 709.0	.00020	.345	.146	.237-11	-26532.	-28.7	.33
	623.0- 661.0	.00020	.345	.146	.275+05	22079.	-28.7	.33
	591.0- 623.0	.00020	.345	.146	.394-12	-25933.	50.9	.33
	473.0- 591.0	.00020	.345	.146	.233+05	19435.	107.5	.33
3 LS 200								
	876.6- 923.0	.00020	.300	.120	.117-04	-3857.	.5	.33
	766.6- 876.6	.00020	.300	.120	.717-10	-24770.	9.6	.33
	723.0- 766.6	.00020	.300	.120	.517+02	16818.	-8.4	.33
	698.0- 723.0	.00020	.300	.120	.104-03	-2020.	-19.1	.33
	673.0- 698.0	.00020	.300	.120	.828-13	-31083.	-16.7	.33
	648.0- 673.0	.00020	.300	.120	.656-02	2475.	-8.4	.33
	623.0- 648.0	.00020	.300	.120	.246+07	27897.	-20.3	.33
	598.0- 623.0	.00020	.300	.120	.161-16	-38180.	7.9	.33
	573.0- 598.0	.00020	.300	.120	.211+08	27800.	71.7	.33
	548.0- 573.0	.00020	.300	.120	.201+00	6772.	24.9	.33
	473.0- 548.0	.00020	.300	.120	.783+04	18279.	54.9	.33
4 PREOX								
	873.0- 908.0	.00034	.300	.620	.542-05	-13061.	.5	.33
	848.0- 873.0	.00034	.300	.620	.855+21	91578.	.5	.33
	748.0- 848.0	.00034	.300	.620	.155+03	18860.	.5	.33
	683.0- 748.0	.00034	.300	.620	.985-02	4500.	-13.9	.33
	623.0- 683.0	.00034	.300	.620	.143-04	-4365.	-13.9	.33
	573.0- 623.0	.00034	.300	.620	.587-02	3085.	-13.9	.33
	498.0- 573.0	.00034	.300	.620	.594+01	10963.	.5	.33
5 PU FOAM								
	644.0- 688.0	.00034	.400	.030	.844+20	65757.	-3.1	.33
	598.0- 644.0	.00034	.400	.030	.617+02	12335.	-11.9	.33
	573.0- 598.0	.00034	.400	.030	.177-01	2646.	2.5	.33
	544.0- 573.0	.00010	.400	.030	.260+06	21435.	2.5	.33
	448.0- 544.0	.00010	.400	.030	.600+01	9900.	.5	.33
6 IMIDE FOAM								
	1006.0- 1073.0	.00010	.200	.023	.306-04	-4763.	.5	.33
	973.0- 1006.0	.00010	.200	.023	.312-13	-46170.	.5	.33
	915.0- 973.0	.00010	.200	.023	.180-06	-16074.	.5	.33
	854.0- 915.0	.00010	.200	.023	.133+02	16862.	-7.3	.33
	796.0- 854.0	.00010	.200	.023	.611-05	-7869.	-7.3	.33
	711.0- 796.0	.00010	.200	.023	.107+08	36705.	-7.0	.33
	673.0- 711.0	.00010	.200	.023	.763-02	6938.	-.3	.33

NORMALIZED FRAGMENT SIZE AT END TEMPS OF KINETIC REGIMES

1	COVER FABR				
		523.2- 602.2	1.000000	--	.821322
		602.2- 689.2	.821322	--	.602183
		689.2- 763.2	.602183	--	.467861
		763.2- 813.2	.467861	--	.193770
		813.2- 848.2	.193770	--	.059566
		848.2- 898.2	.059566	--	.007807
2	VONAR				
		473.0- 591.0	1.000000	--	.865850
		591.0- 623.0	.865850	--	.793600
		623.0- 661.0	.793600	--	.718568
		661.0- 709.0	.718568	--	.644733
		709.0- 766.0	.644733	--	.598173
		766.0- 881.0	.598173	--	.535456
		881.0- 923.0	.535456	--	.522900
3	LS 200				
		473.0- 548.0	1.000000	--	.967082
		548.0- 573.0	.967082	--	.934163
		573.0- 598.0	.934163	--	.871674
		598.0- 623.0	.871674	--	.820223
		623.0- 648.0	.820223	--	.781499
		648.0- 673.0	.781499	--	.725286
		673.0- 698.0	.725286	--	.688495
		698.0- 723.0	.688495	--	.666312
		723.0- 766.6	.666312	--	.615242
		766.6- 876.6	.615242	--	.550394
		876.6- 923.0	.550394	--	.542658
4	PREOX				
		498.0- 573.0	1.000000	--	.953137
		573.0- 623.0	.953137	--	.892503
		623.0- 683.0	.892503	--	.828126
		683.0- 748.0	.828126	--	.763548
		748.0- 848.0	.763548	--	.542460
		848.0- 873.0	.542460	--	.367852
		873.0- 908.0	.367852	--	.146867
5	PU FOAM				
		448.0- 544.0	1.000000	--	.918893
		544.0- 573.0	.918883	--	.834678
		573.0- 598.0	.834678	--	.727952
		598.0- 644.0	.727952	--	.490399
		644.0- 688.0	.490399	--	.006318
6	IMIDE FOAM				
		673.0- 711.0	1.000000	--	.994404
		711.0- 796.0	.994404	--	.917053
		796.0- 854.0	.917053	--	.803906
		854.0- 915.0	.803906	--	.679453
		915.0- 973.0	.679453	--	.574808
		973.0- 1006.0	.574808	--	.546754
		1006.0- 1073.0	.546754	--	.513983

RUN NO. 18 0.5-INCH LS-200 (T=6 MIN)

MATERIAL / THICKNESS

COVER FABR .1 CM

LS 200 1.3 CM

PU FOAM 10.0 CM

BOUNDARY CONDITION
HEAT FLUX (CONDUCTIVE) = .0400 CAL/CM2.SEC
SURFACE TEMPERATURE = 691.0 K

I	RB	TS(I) - TS(I+1)	DX	X(I) - X(I+1)	QS(I)	QS(I+1)	N(I)	N(I+1)
1 COVER FABR								
1	.00084	691.0 -- 689.2	.00	.0000- .0045	.0400	.0398	.59942	.60218
2	.00084	689.2 -- 685.2	.01	.0045- .0145	.0398	.0395	.60218	.60837
3	.00084	685.2 -- 681.2	.01	.0145- .0247	.0395	.0391	.60837	.61480
4	.00085	681.2 -- 677.2	.01	.0247- .0349	.0391	.0387	.61480	.62149
5	.00086	677.2 -- 673.2	.01	.0349- .0452	.0387	.0383	.62149	.62844
6	.00087	673.2 -- 669.2	.01	.0452- .0557	.0383	.0380	.62844	.63569
7	.00087	669.2 -- 665.2	.01	.0557- .0662	.0380	.0376	.63568	.64323
8	.00088	665.2 -- 661.2	.01	.0662- .0769	.0376	.0372	.64323	.65109
9	.00089	661.2 -- 657.2	.01	.0769- .0876	.0372	.0368	.65109	.65929
10	.00090	657.2 -- 653.2	.01	.0876- .0985	.0368	.0364	.65929	.66785
11	.00091	653.2 -- 652.6	.00	.0985- .1000	.0364	.0364	.66785	.66909
2 LS 200								
12	.00183	652.6 -- 648.6	.02	.1000- .1220	.0364	.0361	.77106	.78006
13	.00184	648.6 -- 648.0	.00	.1220- .1255	.0361	.0361	.78006	.78150
14	.00184	648.0 -- 644.0	.02	.1255- .1477	.0361	.0359	.78150	.78997
15	.00185	644.0 -- 640.0	.02	.1477- .1700	.0359	.0357	.78997	.79744
16	.00186	640.0 -- 636.0	.02	.1700- .1924	.0357	.0354	.79744	.80401
17	.00187	636.0 -- 632.0	.02	.1924- .2150	.0354	.0352	.80401	.80978
18	.00189	632.0 -- 628.0	.02	.2150- .2378	.0352	.0349	.80978	.81482
19	.00190	628.0 -- 624.0	.02	.2378- .2607	.0349	.0347	.81482	.81922
20	.00191	624.0 -- 623.0	.01	.2607- .2664	.0347	.0346	.81922	.82022
21	.00192	623.0 -- 619.0	.02	.2664- .2896	.0346	.0343	.82022	.82460
22	.00194	619.0 -- 615.0	.02	.2896- .3129	.0343	.0340	.82460	.82998
23	.00195	615.0 -- 611.0	.02	.3129- .3364	.0340	.0337	.82998	.83663
24	.00197	611.0 -- 607.0	.02	.3364- .3601	.0337	.0334	.83663	.84487
25	.00199	607.0 -- 603.0	.02	.3601- .3840	.0334	.0331	.84487	.85513
26	.00201	603.0 -- 599.0	.02	.3840- .4082	.0331	.0328	.85513	.86797
27	.00203	599.0 -- 598.0	.01	.4082- .4143	.0328	.0327	.86797	.87167
28	.00204	598.0 -- 594.0	.02	.4143- .4387	.0327	.0322	.87167	.88595
29	.00207	594.0 -- 590.0	.02	.4387- .4635	.0322	.0317	.88595	.89831
30	.00210	590.0 -- 586.0	.03	.4635- .4888	.0317	.0312	.89831	.90898
31	.00214	586.0 -- 582.0	.03	.4888- .5145	.0312	.0307	.90898	.91814
32	.00217	582.0 -- 578.0	.03	.5145- .5405	.0307	.0302	.91814	.92597
33	.00220	578.0 -- 574.0	.03	.5405- .5670	.0302	.0298	.92597	.93266
34	.00223	574.0 -- 573.0	.01	.5670- .5737	.0298	.0297	.93266	.93416
35	.00224	573.0 -- 569.0	.03	.5737- .6006	.0297	.0293	.93416	.93996
36	.00227	569.0 -- 565.0	.03	.6006- .6279	.0293	.0290	.93996	.94555
37	.00229	565.0 -- 561.0	.03	.6279- .6555	.0290	.0286	.94555	.95094
38	.00232	561.0 -- 557.0	.03	.6555- .6835	.0286	.0282	.95094	.95612
39	.00235	557.0 -- 553.0	.03	.6835- .7118	.0282	.0279	.95612	.96111

40	.00238	553.0 -- 549.0	.03	.7118-	.7405	.0279	.0275	.96111	.96591
41	.00242	549.0 -- 548.0	.01	.7405-	.7478	.0275	.0274	.96591	.96708
42	.00243	548.0 -- 544.0	.03	.7478-	.7770	.0274	.0270	.96708	.97148
43	.00246	544.0 -- 540.0	.03	.7770-	.8067	.0270	.0265	.97148	.97538
44	.00251	540.0 -- 536.0	.03	.8067-	.8369	.0265	.0261	.97538	.97883
45	.00254	536.0 -- 532.0	.03	.8369-	.8675	.0261	.0257	.97883	.98187
46	.00259	532.0 -- 528.0	.03	.8675-	.8986	.0257	.0253	.98187	.98455
47	.00263	528.0 -- 524.0	.03	.8986-	.9302	.0253	.0249	.98455	.98691
48	.00268	524.0 -- 520.0	.03	.9302-	.9624	.0249	.0244	.98691	.98897
49	.00272	520.0 -- 516.0	.03	.9624-	.9951	.0244	.0240	.98897	.99078
50	.00277	516.0 -- 512.0	.03	.9951-	1.0284	.0240	.0236	.99078	.99236
51	.00282	512.0 -- 508.0	.03	1.0284-	1.0623	.0236	.0232	.99236	.99373
52	.00287	508.0 -- 504.0	.03	1.0623-	1.0968	.0232	.0227	.99373	.99492
53	.00293	504.0 -- 500.0	.04	1.0968-	1.1320	.0227	.0223	.99492	.99595
54	.00299	500.0 -- 496.0	.04	1.1320-	1.1679	.0223	.0218	.99595	.99684
55	.00305	496.0 -- 492.0	.04	1.1679-	1.2046	.0218	.0214	.99684	.99761
56	.00311	492.0 -- 488.0	.04	1.2046-	1.2420	.0214	.0209	.99761	.99827
57	.00318	488.0 -- 484.0	.04	1.2420-	1.2802	.0209	.0205	.99827	.99883
58	.00325	484.0 -- 480.0	.04	1.2802-	1.3193	.0205	.0200	.99883	.99932
59	.00333	480.0 -- 476.0	.04	1.3193-	1.3593	.0200	.0195	.99932	.99973
3 PU FOAM									
60	.00172	476.0 -- 472.0	.02	1.3593-	1.3799	.0195	.0194	.98945	.99140
61	.00172	472.0 -- 468.0	.02	1.3799-	1.4005	.0194	.0193	.99140	.99318
62	.00172	468.0 -- 464.0	.02	1.4005-	1.4212	.0193	.0192	.99318	.99480
63	.00173	464.0 -- 460.0	.02	1.4212-	1.4420	.0192	.0192	.99480	.99629
64	.00173	460.0 -- 456.0	.02	1.4420-	1.4628	.0192	.0191	.99629	.99765
65	.00174	456.0 -- 452.0	.02	1.4628-	1.4838	.0191	.0190	.99765	.99888
66	.00175	452.0 -- 448.0	.02	1.4838-	1.5049	.0190	.0189	.99888	1.00000
67	.00967	448.0 -- 444.0	.02	1.5049-	1.5260	.0189	.0184	1.00000	1.00000
68	.00967	444.0 -- 440.0	.02	1.5260-	1.5477	.0184	.0180	1.00000	1.00000
69	.00967	440.0 -- 436.0	.02	1.5477-	1.5700	.0180	.0175	1.00000	1.00000
70	.00967	436.0 -- 432.0	.02	1.5700-	1.5928	.0175	.0171	1.00000	1.00000
71	.00967	432.0 -- 428.0	.02	1.5928-	1.6162	.0171	.0166	1.00000	1.00000
72	.00967	428.0 -- 424.0	.02	1.6162-	1.6404	.0166	.0161	1.00000	1.00000
73	.00967	424.0 -- 420.0	.02	1.6404-	1.6652	.0161	.0157	1.00000	1.00000
74	.00967	420.0 -- 416.0	.03	1.6652-	1.6907	.0157	.0152	1.00000	1.00000
75	.00967	416.0 -- 412.0	.03	1.6907-	1.7170	.0152	.0147	1.00000	1.00000
76	.00967	412.0 -- 408.0	.03	1.7170-	1.7442	.0147	.0143	1.00000	1.00000
77	.00967	408.0 -- 404.0	.03	1.7442-	1.7722	.0143	.0138	1.00000	1.00000
78	.00967	404.0 -- 400.0	.03	1.7722-	1.8012	.0138	.0133	1.00000	1.00000
79	.00967	400.0 -- 396.0	.03	1.8012-	1.8312	.0133	.0129	1.00000	1.00000
80	.00967	396.0 -- 392.0	.03	1.8312-	1.8622	.0129	.0124	1.00000	1.00000
81	.00967	392.0 -- 388.0	.03	1.8622-	1.8945	.0124	.0119	1.00000	1.00000
82	.00967	388.0 -- 384.0	.03	1.8945-	1.9279	.0119	.0115	1.00000	1.00000
83	.00967	384.0 -- 380.0	.03	1.9279-	1.9628	.0115	.0110	1.00000	1.00000
84	.00967	380.0 -- 376.0	.04	1.9628-	1.9991	.0110	.0106	1.00000	1.00000
85	.00967	376.0 -- 372.0	.04	1.9991-	2.0370	.0106	.0101	1.00000	1.00000
86	.00967	372.0 -- 368.0	.04	2.0370-	2.0766	.0101	.0096	1.00000	1.00000
87	.00967	368.0 -- 364.0	.04	2.0766-	2.1181	.0096	.0092	1.00000	1.00000
88	.00967	364.0 -- 360.0	.04	2.1181-	2.1618	.0092	.0087	1.00000	1.00000
89	.00967	360.0 -- 356.0	.05	2.1618-	2.2078	.0087	.0082	1.00000	1.00000
90	.00967	356.0 -- 352.0	.05	2.2078-	2.2563	.0082	.0078	1.00000	1.00000
91	.00967	352.0 -- 348.0	.05	2.2563-	2.3078	.0078	.0073	1.00000	1.00000
92	.00967	348.0 -- 344.0	.05	2.3078-	2.3625	.0073	.0068	1.00000	1.00000
93	.00967	344.0 -- 340.0	.06	2.3625-	2.4210	.0068	.0064	1.00000	1.00000
94	.00967	340.0 -- 336.0	.06	2.4210-	2.4837	.0064	.0059	1.00000	1.00000
95	.00967	336.0 -- 332.0	.07	2.4837-	2.5513	.0059	.0055	1.00000	1.00000

96	.00967	332.0 -- 328.0	.07	2.5513-	2.6246	.0055	.0050	1.00000	1.00000
97	.00967	328.0 -- 324.0	.09	2.6246-	2.7048	.0050	.0045	1.00000	1.00000
98	.00967	324.0 -- 320.0	.09	2.7048-	2.7932	.0045	.0041	1.00000	1.00000
99	.00967	320.0 -- 316.0	.10	2.7932-	2.8917	.0041	.0036	1.00000	1.00000
100	.00967	316.0 -- 312.0	.11	2.8917-	3.0030	.0036	.0031	1.00000	1.00000
101	.00967	312.0 -- 308.0	.13	3.0030-	3.1307	.0031	.0027	1.00000	1.00000
102	.00967	308.0 -- 304.0	.15	3.1307-	3.2806	.0027	.0022	1.00000	1.00000
103	.00967	304.0 -- 300.0	.18	3.2806-	3.4621	.0022	.0017	1.00000	1.00000
104	.00967	300.0 -- 296.0	.23	3.4621-	3.6920	.0017	.0013	1.00000	1.00000
105	.00967	296.0 -- 292.0	.31	3.6920-	4.0054	.0013	.0008	1.00000	1.00000
106	.00967	292.0 -- 288.0	.49	4.0054-	4.4980	.0008	.0003	1.00000	1.00000
107	.00967	288.0 -- 285.0	.86	4.4980-	5.3600	.0003	.0000	1.00000	1.00000

MASS LOSS FOR 1 LAYER= .2420-04
2 LAYER= .5851-04

3 LAYER= .5464-06

***** TOTAL MASS LOSS = .8325-04 GM/SEC.CM2 OF BURNING SURFACE

APPENDIX C Some Comments on Burning Tests Procedure

The burning tests of multi-layered seat cushion assemblies were conducted in an NBS Smoke Density Chamber. The orginial radiative heat source is replaced by a Mellen furnace Model 10, to provide a high heat flux, and further supplemented with a cantilever beam coupled to a transducer, to measure weight changes of suspended samples.

In addition to these, there were several modifications on the procedures of sample preparation and it's burning. These were instated following the detection of unsatisfactory conditions during the initial trial runs. These are summarized below.

Symptom	Diagnosis	Remedy
A) Uneven heating (Severe 2-D effect)	1. Misalignment of sample with furnace	1. Align correctly
	2. Use of stainless steel fram as sample holder	2. Eliminate the frame, i.e., large heat sink item
	3. Loss of heat on four sides	3. Use of light, thick insulator on four sides, also as sample holder
	4. Buoyancy of hot gas formed in foam (open cell)	4. No remedy unless sample positioned horizontally
B) Irregular surface shape (or disengaging the cover sheet in the worst case)	High pressure exerted by the gas product during intumescence	Cover fabric cut larger than the surface area, folded over the sides and stapled
C) Temperature rise at the sample surface before removing	Single sheet of radiation shield -- not enough	Use double layers (with air-gap in between) of shields

Symptom	Diagnosis	Remedy
D) Furnace temperature change on and after removing the shield	Change in Characteristics of reradiation from the shield and the sample surface	Adjust the power to the furnace manually to maintain the same furnace temperature
E) Non-linear signal response of transducer	Electronic feature of the equipment used	Make and use a calibration chart
F) Irreproducible weight measurement of sample	Irregularly distributed loading on the cantilever beam	Hold the entire sample by a single wire and load it at the fixed point of the beam
G) Step changes in weight measurement during the burning	Interference by the thermocouples inserted into the sample	Duplicate the run without thermocouples purely for weight change measurement

APPENDIX D Photographs of Equipments and Burned Samples

Photo No.	Remarks

1. **Thermogravimetric Analyzer (TG)**
The thermogravimetric analyzer is shown in the right side of the picture, connected to a pair of flowmeters and a mixer, plus a vacuum gauge (vacuum pump not shown). The assemblage of a chart recorder, a microprocessor, a heater controller, and a weight suppressor are shown in the left side on the table.

2. **Differential Scanning Calorimeter (DSC)**
The DSC is shown here with a SAZ (Scanning Auto Zero) on its top. The sample heater unit is located on the deck on the left side. The DSC is not used extensively in this work.

3. **NBS Smoke Density Chamber**
The NBS Smoke Density Chamber is shown at left rear. A newly installed Mellen furnace is seen through its window. The multichannel recorder (Leeds & Northrop, Speedomax Model 251) is shown at the top of the front cabinet.

4. **Sample Preparation**
This picture shows each seat cushion sample is prepared for the burning tests in the NBS Smoke Density Chamber. The front cover fabric is cut larger than the face area and folded over the sides and stapled. The entire sample is surrounded by four 1"-thick insulator panels (Kaowood-3000° Board, by Pyroengineering Co.).

5. **Sample Arrangement Inside of the NBS Smoke Density Chamber**
Eight pairs of thermocouple (Pt vs. Pt-10% Rh) wires are shown here penetrating into the seat cushion assemblage, which is suspended by a cantilever beam. The beam is a part of a transducer-type weight measuring device. The Mellen furnace is shown at the lower left corner.

6. **Visual Comparison of the Burned Seat Cushions**
Each seat cushion system was suddenly exposed to the Mellen furnace preheated and maintained at 850°C and then remained so for 10 minutes. This pictures shows that the effectiveness of the fire blocking layer can be rated, based on this test only, in decreasing order: LS-200 (1/2" thick) > Vonar (3/16" thick) > Preox (11 oz/yd^2) > No blocking layer.

7. **Comparison of the Degree of In-Depth Burning**
Same as above, but this picture shows the degree of in-depth burning, with the samples oriented in the same way as in the NBS Smoke Density Chamber.

8. **Comparison of LS-200 and Vonar as a Fire Blocking Layer**
In this picture, LS-200 is shown more effective as a fire blocking layer than Vonar when tested with the same thickness.

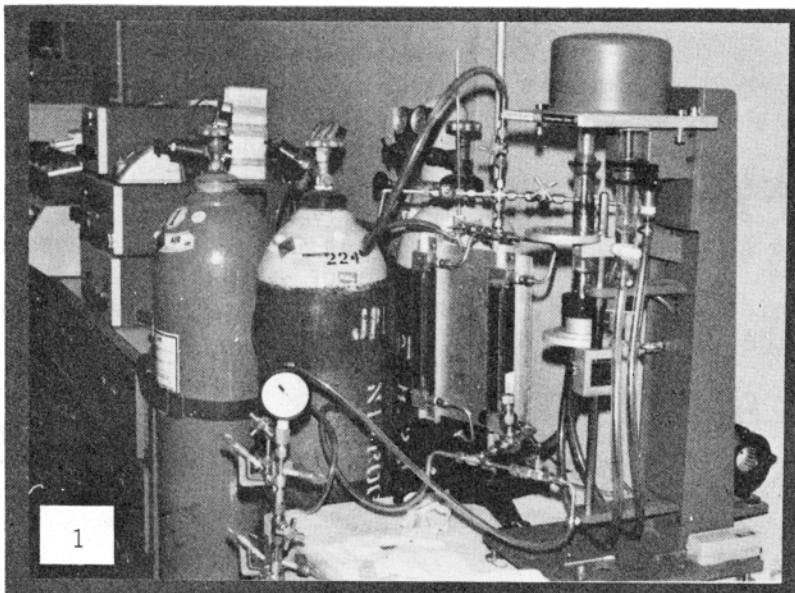

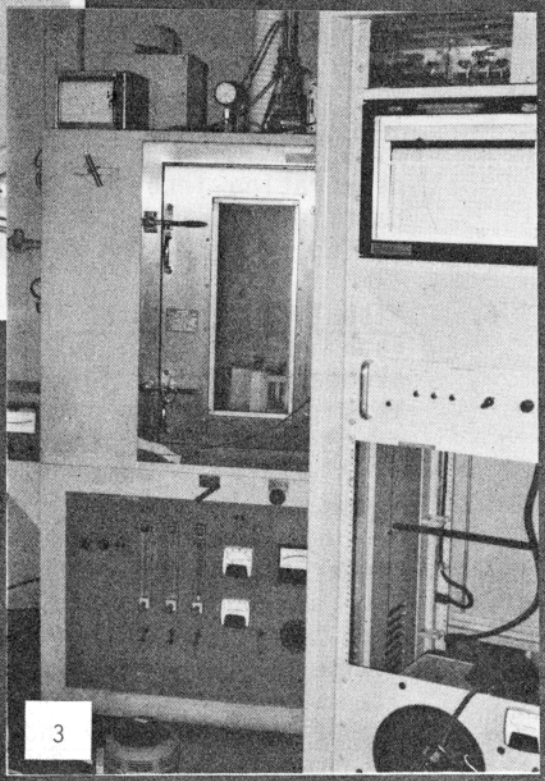

D2

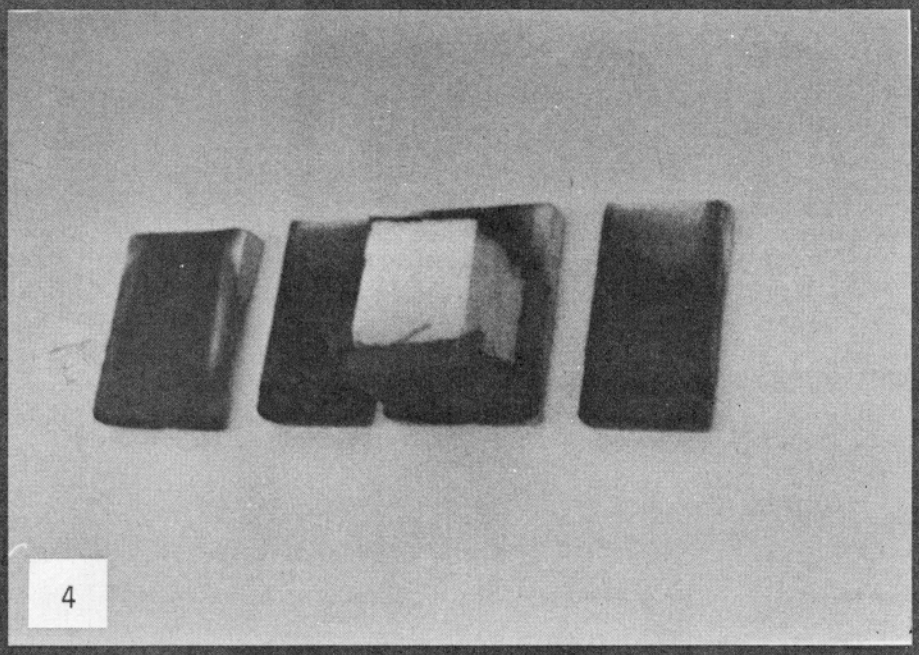

4

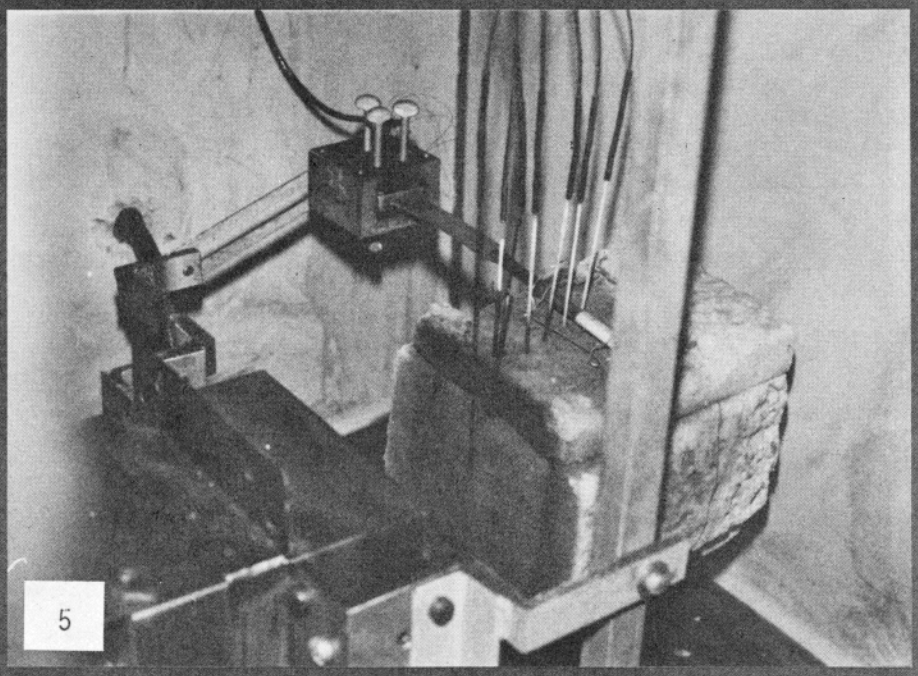

5

D3

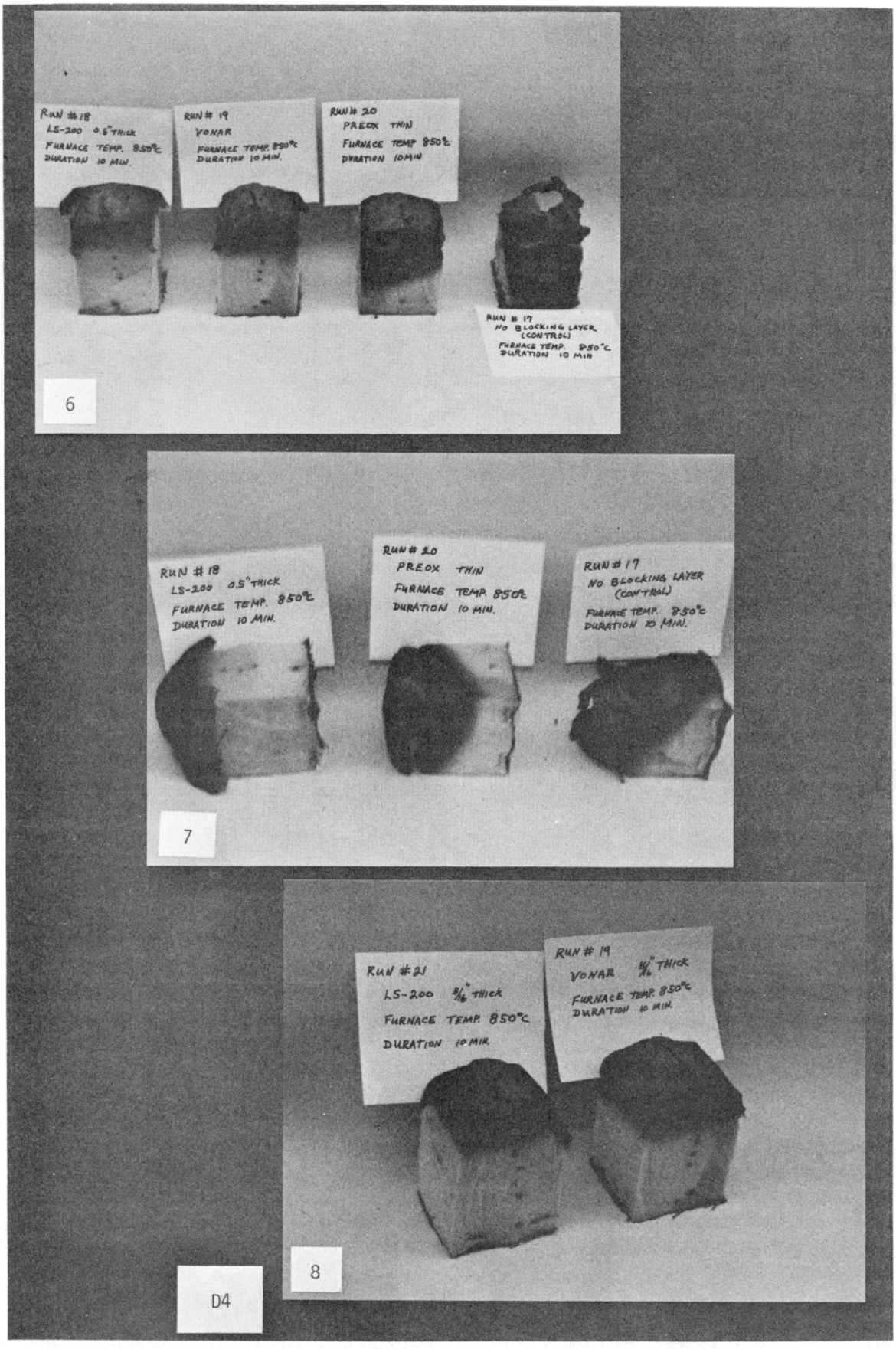
RUN #18
LS-200 0.5" THICK
FURNACE TEMP. 850°C
DURATION 10 MIN.
RUN # 19
VONAR
FURNACE TEMP. 850°C
DURATION 10 MIN.
RUN # 20
PREOX THIN
FURNACE TEMP 850°C
DURATION 10MIN
RUN # 17
NO BLOCKING LAYER
(CONTROL)
FURNACE TEMP. 850°C
DURATION 10 MIN
6
RUN #18
LS-200 0.5" THICK
FURNACE TEMP. 850°C
DURATION 10 MIN.
RUN # 20
PREOX THIN
FURNACE TEMP. 850°C
DURATION 10 MIN.
RUN # 17
NO BLOCKING LAYER
(CONTROL)
FURNACE TEMP. 850°C
DURATION 10 MIN.
7
RUN #21
LS-200 5/16" THICK
FURNACE TEMP. 850°C
DURATION 10 MIN.
RUN # 19
VONAR 5/16" THICK
FURNACE TEMP. 850°C
DURATION 10 MIN.
8
D4

B) Dimensional Analysis

The dimensional analyses are performed for these two models to determine their relative strengths and shortcomings. The dimensionless groups needed to describe these models, according to Pi theorem, could be the following:

Dimensionless Group	JPL's TCM	FMC's NM
Temperature	$\frac{T - T_o}{T_s - T_o}$	$\frac{T - T_o}{T_s - T_o}$
Distance Coordinate	$\frac{\rho rcx}{k}$	$\frac{M_g cx}{k}$
Heat of Pyrolysis	$\frac{D}{c(T_s - T_o)}$	$\frac{Q}{c(T_s - T_o)}$
Arrhenius Group (or Activation Temperature)	$\frac{E}{RT}$	$\frac{E}{RT}$
Preexponential Factor	$\frac{Bx}{r}$	Bt
Fourier Number	-	$\frac{kt}{\rho_c x^2}$

The obvious difference is that Fourier number, which compares a characteristic length dimension with an approximate temperature-wave penetration depth for a given time t, is included in the NM while it is absent in TCM. Other than the capability of the NM to study unsteady-state behavior, essentially the same dimensionless groups are required for the analysis of the two models.

C) Input Data

	TCM	NM
C_p, k	1. For one solid 2. Stepwise variation with temperature	1. For two solids (active material and char) and one C_p for gas 2. Linear variation with temperature
ρ	Stepwise variation with temperature	The initial and final densities (char fraction increases linearly from 0 to 100% of apparent density)
B, E	Change often (as evidenced by TGA) depending on temperature range	One set of constant values for the whole temperature range
Heat sink term	D: heat of degradation stepwise variation with temperature (to be obtained from DSC)	Q: heat of pyrolysis fixed at a reference temperature
Boundary Conditions	1. Temperature B.C.'s at both boundaries or 2. Temperature and heat flux B.C.'s at one boundary	Either temperature or heat flux B.C. at each of two boundaries

D) Calculation & Results

	TCM	NM
Calculation	Segment-wise application of analytical solution, progressively advancing from one boundary to the other	Finite difference representations of the partial differential equation for the entire region and solving the resultant tridiagonal matrix
Results	surface regression rate, temperature profile and total mass loss	temperature profile, density profile, and mass flux profile

E) Advantages & Disadvantages

	TCM	NM
Advantage	Parametric analysis is readily accessible - essential for basics understanding and establishing design criteria	Time-dependent pyrolysis behavior can be predicted (This may be useful for assuming and confirming time-dependent boundary conditions more realistically.)
Disadvantage	Steady state solution is not adequate for study of transient period	Parametric analysis may be not as clear as TCM